

AD-A074 635

BATTELLE MEMORIAL INST COLUMBUS OHIO
ARC-TUNNEL STAGNATION ENTHALPY MEASUREMENTS UTILIZING THE COPPE--ETC(U)
JUN 79 A A BOIARSKI

F/G 14/2

F33615-76-C-3145

UNCLASSIFIED

AFFDL-TR-79-3068

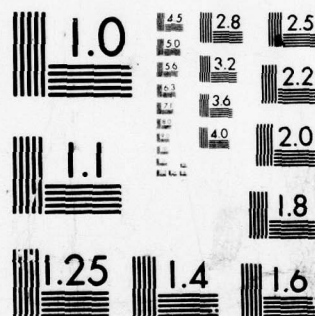
NL

/ OF \

AD
A074635



END
DATE
FILMED
11-79
DDC



MICROCOPY RESOLUTION TEST CHART
NATIONAL BUREAU OF STANDARDS-1963-A

AD A074635

DDC FILE COPY

AFFDL-TR-79-3068

1
2
15

LEVEL 7

**ARC-TUNNEL STAGNATION ENTHALPY
MEASUREMENTS UTILIZING THE
COPPER-LINE-RATIO METHOD CORRECTED
FOR SELF-ABSORPTION EFFECTS**

*BATTELLE MEMORIAL INSTITUTE
505 KING AVENUE
COLUMBUS, OHIO 43201*

JUNE 1979

TECHNICAL REPORT AFFDL-TR-79-3068
Final Report for Period November 1977 Through October 1978

DDC
RECEIVED
OCT 4 1979
A

Approved for public release; distribution unlimited.

AIR FORCE FLIGHT DYNAMICS LABORATORY
AIR FORCE WRIGHT AERONAUTICAL LABORATORIES
AIR FORCE SYSTEMS COMMAND
WRIGHT-PATTERSON AIR FORCE BASE, OHIO 45433

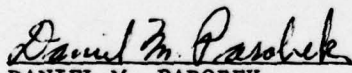
79 10 04 009


NOTICE

When Government drawings, specifications, or other data are used for any purpose other than in connection with a definitely related Government procurement operation, the United States Government thereby incurs no responsibility nor any obligation whatsoever; and the fact that the Government may have formulated, furnished, or in any way supplied the said drawings, specifications, or other data, is not to be regarded by implication or otherwise as in any manner licensing the holder or any other person or corporation, or conveying any rights or permission to manufacture, use, or sell any patented invention that may in any way be related thereto.

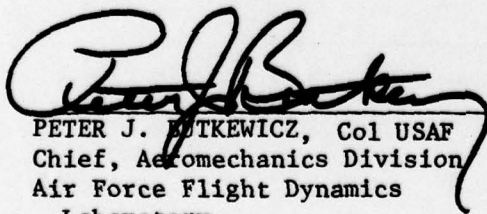
This report has been reviewed by the Information Office (IO) and is releasable to the National Technical Information Service (NTIS). At NTIS, it will be available to the general public, including foreign nations.

This technical report has been reviewed and is approved for publication.


DANIEL M. PAROBEC
Technical Manager, Experimental
Engineering Branch


ROBERT G. DUNN
Chief, Experimental Engineering
Branch

FOR THE COMMANDER


PETER J. BUTKEWICZ, Col USAF
Chief, Aeromechanics Division
Air Force Flight Dynamics
Laboratory

Copies of this report should not be returned unless return is required by security considerations, contractual obligations, or notice on a specific document.

UNCLASSIFIED

SECURITY CLASSIFICATION OF THIS PAGE (When Data Entered)

19 REPORT DOCUMENTATION PAGE		READ INSTRUCTIONS BEFORE COMPLETING FORM
1. REPORT NUMBER AFFDL-TR-79-3068	2. GOVT ACCESSION NO.	3. RECIPIENT'S CATALOG NUMBER
4. TITLE (and Subtitle) Arc-Tunnel Stagnation Enthalpy Measurements Utilizing the Copper-Line-Ratio Method Corrected for Self-Absorption Effects		5. TYPE OF REPORT & PERIOD COVERED Final Technical Rept. Nov 1977 - Oct 1978
6. AUTHOR(s) Anthony A. Boiarski	7. PERFORMING ORG. REPORT NUMBER	
8. PERFORMING ORGANIZATION NAME AND ADDRESS Battelle Memorial Institute 505 King Avenue Columbus, Ohio 43201	9. CONTRACT OR GRANT NUMBER(s) F33615-76-C-3145	
10. CONTROLLING OFFICE NAME AND ADDRESS Air Force Flight Dynamics Laboratory (FXN) Wright-Patterson AFB, Ohio 45433	11. PROGRAM ELEMENT, PROJECT, TASK AREA & WORK UNIT NUMBERS Prog Element 62201F, Project 2404, Task 240413, Work Unit 24041302	
12. MONITORING AGENCY NAME & ADDRESS (if different from Controlling Office) 1266	13. REPORT DATE June 1979	
14. DISTRIBUTION STATEMENT (of this Report) Approved for public release; distribution unlimited.	15. NUMBER OF PAGES 56	
15. DISTRIBUTION STATEMENT (of the abstract entered in Block 20, if different from Report)	16. SECURITY CLASS. (of this report) Unclassified	
17. DECLASSIFICATION/DOWNGRADING SCHEDULE		
18. SUPPLEMENTARY NOTES		
19. KEY WORDS (Continue on reverse side if necessary and identify by block number) Arc tunnel Self-absorption Flow enthalpy Line shift Copper density Line broadening Copper lines		
20. ABSTRACT (Continue on reverse side if necessary and identify by block number) Detailed measurements of the copper emission spectrum at 5106 Å and 5153 Å were obtained while observing radiation from the free-stream and model nose-cap regions of an arc-heated wind tunnel flow. The ratio of peak line intensities and the absolute width of the 5106 Å line were used to infer gas temperature (i.e., enthalpy) and copper density corrected for self-absorption effects. Line shift measurements were also obtained in order to corroborate the use of Lindholm's collision broadening theory in the		

DD FORM 1 JAN 73 1473

EDITION OF 1 NOV 65 IS OBSOLETE

UNCLASSIFIED

SECURITY CLASSIFICATION OF THIS PAGE (When Data Entered)

052 400

JP

UNCLASSIFIED

SECURITY CLASSIFICATION OF THIS PAGE(When Data Entered)

20. self-absorption analysis. Final enthalpy results for the peaked profile mode of operation indicated that a significant correction to measured enthalpy resulted when self-absorption was taken into account. The resulting average stagnation enthalpy value of 5250 Btu/lbm was in good agreement with previously obtained results utilizing a combined heat flux and pitot probe technique.

UNCLASSIFIED

SECURITY CLASSIFICATION OF THIS PAGE(When Data Entered)

FOREWORD

This report was prepared as part of a contract effort conducted by Dr. Anthony A. Boiarski of Battelle Memorial Institute, Columbus, Ohio. The performance period was from November 1977 through September 1978. The work was performed under a visiting scientist arrangement through the University of Dayton under task number 33 of Air Force Contract F33615-76-C-3145. The test and systems development phases of this work were carried out jointly with Air Force Flight Dynamics Laboratory, Experimental Engineering Branch (AFFDL/FXN) personnel. The work was an element of in-house work unit 24041302, "Real Gas Diagnostics and Similitude" of task 240413, "Aerodynamic Ground Test Technology."

Mr. Daniel M. Parobek of AFFDL/FXN was contract monitor and in-house work unit engineer manager. Mr. Henry Baust of this same Branch was the electronics engineer.

The author and Mr. Parobek wish to acknowledge the efforts of Mr. Hsue-Fu Lee of AFFDL for his past contributions on the copper-line-ratio project which led to the work reported here. They also wish to acknowledge the preceding copper-line-ratio project breakthroughs accomplished by Mr. Jon Bader, formerly of the Flight Dynamics Laboratory, whose published and unpublished work served as a starting point for the present study.

Accession For	
NTIS G&A&I	<input checked="checked" type="checkbox"/>
DDC TAB	<input type="checkbox"/>
Unannounced	<input type="checkbox"/>
Justification	
By _____	
Distribution/	
Availability Codes	
Dist..	Availand/or special
A	

TABLE OF CONTENTS

SECTION		PAGE
I	INTRODUCTION	1
II	EXPERIMENTAL SETUP	5
III	ARC-FACILITY TESTING	11
	A. Calibration	11
	B. Preliminary Tests	14
	C. RENT Tests.	14
IV	DATA REDUCTION PROCEDURE	18
	A. General	18
	B. Theory for Self-Absorption Corrections.	25
	C. Example Calculations.	31
V	EXPERIMENTAL RESULTS AND DISCUSSION.	32
	A. Temperature and Enthalpy.	32
	B. Copper Density.	34
	C. Free-Stream Radiation	37
	D. Line Shift.	40
	E. Detailed Line Shape	43
	F. Polychromator Considerations.	49
VI	SUMMARY AND CONCLUSIONS.	52
	REFERENCES	56

LIST OF ILLUSTRATIONS

FIGURE		PAGE
1	Block Diagram of Experimental Setup	6
2	Light Collection and Transfer System.	7
3	Image Transfer and Calibration System	8
4	Variation in Sensitivity Across the Optical Multichannel Analyzer (OMA) Screen from Standard Lamp Calibration	12
5	Flow Chart Describing Data Reduction Procedure for Obtaining Temperature and Copper Density from the Raw Spectral Measurements.	19
6	Optical Multichannel Analyzer (OMA) Scans for Calibration and Test Conditions (Run No. 91-020).	20
7	OMA Data Records for Calibration and Free-Stream Conditions During Run No. 91-029.	23
8	OMA Data Records for Calibration and Model Gas-Cap Conditions During Run No. 91-029.	24
9	Actual Theoretical 5106 to 5153 Å Line Intensity Ratio and 5106 Å Line Full-Width as a Function of Temperature and Copper Density for Conditions of Run No. 91-029 and 91-030 ($p = 80$ atm, $l = 2$ cm, $\gamma_A = 0.98$ Å, $\gamma_{A_2} = 0.80$ Å).	28
10	Theoretical Curves Used to Reduce Measured Line Intensity Ratio and Line Width Data in Order to Obtain Simultaneous Temperature and Copper Density Results for Run No. 91-029 and 91-030 ($p = 80$ atm, $l = 2$ cm, $\gamma_{A_1} = 0.98$ Å, $\gamma_{A_2} = 0.80$ Å).	29
11	Free-Stream and Model Stagnation Temperature Results for Various Arc-Tunnel Runs	33
12	Copper Density Data Obtained for Free-Stream and Model Stagnation Conditions During Several Arc-Tunnel Runs	36
13	Line Shift Data for Various Arc-Tunnel Runs Which were Used to Infer Broadening Constants for the Copper Lines of Interest.	42

LIST OF ILLUSTRATIONS (Continued)

FIGURE		PAGE
14	Comparison of OMA Data Scans with Theory for Free-Stream Versus Model Stagnation Conditions.	46
15	Comparison of OMA Data Scans with Theory for Typical Model Stagnation Conditions	47
16	Indication of Polychromator Performance for Average Line Shift and Shape Conditions During Runs 91-029 and 91-030	50

LIST OF TABLES

TABLE		PAGE
1	Tunnel Test Conditions.	15
2	Experimental Parameters for Various Tunnel Runs	16
3	Average Free-Stream and Model Gas-Cap Temperature Results from All Tunnel Data Compared to Theory for Present Nozzle Flow Conditions	35
4	Broadening Constants Determined from Shift Data for Each Tunnel Run.	44
5	Average Broadening Constants Determined from All Arc-Tunnel Data Compared to Values Determined by Other Authors	45

LIST OF SYMBOLS

C_6	Line broadening constant due to Vander Waals effect (cm^6/sec)
H_0	Stagnation enthalpy (Btu/lbm)
I_i	Value of the peak copper line intensity for a given line at wavelength λ_i
$\int I_i$	Value of the integrated line intensity for a given copper line at wavelength λ_i
l	Length of the radiating slab of high-temperature gas containing copper atoms (cm)
N_{Cu}	Number density of copper (atoms/ cm^3)
N_{N_2}	Number density of nitrogen (molecules/ cm^3)
p	Pressure (atmospheres)
p_0	Arc-tunnel stagnation pressure (atmospheres)
T	Temperature ($^{\circ}\text{K}$)
T_0	Arc-tunnel stagnation temperature ($^{\circ}\text{K}$)

Greek

γ_A	Instrument apparatus function full-width at half-height (\AA) (i.e., Gaussian shape)
γ	True line full-width at half-height independent of line shape (\AA)
γ_m	Measured line full-width at half-height (i.e., convolution of true line profile and instrument apparatus function) (\AA)
Δ	Line shift from zero pressure condition (i.e., positive values indicate a shift toward the blue end of the spectrum) (\AA)
λ_i	Wavelength of line i (\AA)

I. INTRODUCTION

The Air Force Flight Dynamics Laboratory (AFFDL) has developed ground-based facilities capable of simulating the environment experienced by nose tips of reentry vehicles. The AFFDL Reentry Nose Tip (RENT) Facility is such a device which employs an electric arc to heat the test gas. In order to utilize this facility to its greatest potential, the characteristic flow properties must be adequately defined, especially the stagnation enthalpy, H_0 . Attempts have been made to insert physical probes into the flow to measure this quantity, but they have not been entirely satisfactory due to the very high heating rates encountered in the RENT flow. Furthermore, facilities that generate even higher flow enthalpy than the present N-4 heater in the RENT Facility are being developed at AFFDL. The heating rates produced in these new facilities will increase the difficulty of utilizing physical probes for enthalpy measurements:

An alternate approach, which has received a good deal of attention, is a spectroscopic technique involving measurement of atomic line radiation from copper that is present as a contaminant in the flow. Several in-house exploratory studies have been performed to investigate the use of this technique to measure model gas-cap enthalpy in the RENT Facility. (1-3) Results of these efforts indicated that a simple line intensity ratio method could be used to measure gas temperature (i.e., and infer enthalpy) provided that the following assumptions are made:

- Optically thin gas (i.e., no self-absorption)
- Uniform temperature and copper density along the observation path
- Local Thermodynamic Equilibrium (LTE)
- Constant pressure.

In Reference 1, a scanning spectrometer was used to obtain low resolution spectra of copper emission from a model nose tip over a broad spectral region. The 5106 Å, 5153 Å, and 5218 Å copper lines were ultimately identified as being the most useful spectral features for analysis. However, sequential scans of these lines indicated large fluctuations in the 5153 to 5218 line intensity ratio. Theoretically, this ratio should have remained constant due to the small difference in the upper energy levels of these two

lines. This anomalous observation led to the conclusion that one or both of the following occurred^(2,3):

- The scanning spectrometer was not stopping the action in the flow field (i.e., line intensities were fluctuating faster than the 20 μ sec scan time between spectral lines).
- Copper number density fluctuations, self-absorption effects, or both, were occurring which preferentially changed the intensity of one of the selected lines.

In Reference 2, the first conclusion was tested by monitoring the variation in intensity of the 5106 Å line with time using a monochromator. It was found that one order of magnitude intensity fluctuations occurred in times of 1 millisecond but that only 10-20 percent intensity variations were measured in the 20 μ sec line-to-line scan time frame of the rapid scan spectrometer. These small fluctuations in a single line did not explain the large fluctuations in the 5153/5218 intensity ratio noted in Reference 2.

Continued studies at AFFDL^(3,4) centered around the experimental use of an in-house developed polychromator to make real-time measurements of the 5106 Å and 5153 Å line intensities simultaneously in order to establish if self-absorption, or copper density fluctuations, or both, were responsible for the anomalous spectral results. However, use of the polychromator technique for spectral data acquisition led to further concerns because it could not be precluded that this instrument would distinguish the above effects from the possible existence of intensity fluctuations due to line shape and line shift variations.

Theoretical investigations were also undertaken at AFFDL to supply a method of correcting the line spectra for possible self-absorption effects and to calculate a quantitative error estimate for the line ratio technique^(3,4). This theory computed integrated line intensity only (i.e., no line shape or shift results were computed). Polychromator data utilizing the 5106/5153 line ratio and the absolute intensity of the 5106 Å line were then used in conjunction with the theoretical calculations to show qualitatively that the optically thin assumption was invalid⁽⁴⁾. However, quantitative corrections for self-absorption were hampered by the fact

that line shift and line shape changes were not accounted for in the polychromator intensity measurements.

The main purpose of the study reported herein was to ascertain the quantitative effects of self-absorption, line shift, and shape change on the overall enthalpy measurement utilizing the copper line technique. A secondary objective was to make a proper correction for such effects so that accurate enthalpy results could still be obtained in the RENT environment. Finally, the shift and shape change information were used to check the validity of utilizing the polychromator method for recording the raw line-intensity data.

To accomplish these tasks, a new technique was chosen to obtain copper line spectra. This method involved the use of an optical multichannel analyzer (OMA) which recorded the entire 5106 Å and 5153 Å line spectrum simultaneously. This spectrum was obtained under conditions of high spectral resolution such that line shapes, widths, and line shifts could be determined for the 5106 Å and 5153 Å lines. Furthermore, the spectrum was obtained in a time scale compatible with the requirement for instantaneous measurements (i.e., data gathering times of the order of 10-20 μsec).

Spectral data were collected from graphite model gas caps during three RENT facility peak-enthalpy profile runs at various times and for different experimental conditions. Also, free-stream copper line emission data were obtained for the first time. These combined measurements provided a means of checking the spectroscopically determined static-to-total temperature ratio against thermodynamic calculations based upon the RENT flow environment.

It was found that the simultaneous measurement of the 5106/5153 peak intensity ratio and the full half-width of the 5106 Å line could be used to correct the measured spectrum for self-absorption effects.⁽⁵⁾ Therefore, the theory required to calculate line profile shape, line shift, and line intensity values for this correction procedure was incorporated into the AFFDL copper line computer code. The most recent atomic constants determined by CALSPAN⁽⁶⁾ were utilized in this improved code. This new theory predicted the above spectral parameters (i.e., line width, shift, and peak, as well as integrated line intensities) for an unknown and varying amount of copper in the flow.

Hence, the improved theory and measurement procedures provided the most accurate spectroscopic measure of enthalpy to date. The first quantitative accuracy estimate was also obtained for the self-absorption correction procedure.

Furthermore, line shift information determined in the course of this study was used to compute line broadening constants which could be compared to those determined by other authors. This comparison lends support to the application of Lindholm's line broadening theory to predict the detailed spectrum of the copper lines of interest in the RENT flow environment.

In Section II, the experimental apparatus is described which was used to obtain spectral data for the present study. Arc-tunnel conditions and experimental parameters are given in Section III along with example data taken during the various arc-tunnel runs. In Section IV, the data reduction procedure and sample data reduction calculations are described with reference to the methodology for correcting for self-absorption of the copper line radiation. Discussion of experimental results and conclusions are given in Sections V and VI, respectively.

II. EXPERIMENTAL SETUP

The experimental apparatus used to obtain copper (Cu) line spectra in the RENT facility is shown schematically in Figure 1. Radiation from the model nose cap or nozzle free stream was collected by a 10-cm-focal-length lens, 2.5 cm in diameter. This lens was located 30.5 cm from the model centerline and it focused the collected light onto an 8-mm-diameter coherent fiber-bundle face. A heat reflecting mirror (i.e., "Hot" mirror) was placed in front of this collection lens to minimize heating effects due to radiation from the high-temperature models. A photograph of the light collection system is shown in Figure 2. Note the adjustments available for positioning the point of light collection and setting the lens focus.

The collected radiation was then transferred through 3 meters of the fiber bundle onto the optical rail of a Jarrell-Ash 3/4-meter spectrograph (see Figure 3). Cu line emission exiting the fiber bundle was then collected and focused onto the spectrograph slit with a 13-cm-focal-length, 9.5-cm-diameter lens which was located 46 cm from the slit. An order sorter filter (not shown in Figure 1) was also placed in front of the slit to block light at wavelengths less than 5000 Å. Taking into account entry losses and absorption in the fibers, 25 percent of the initial radiation incident on the collector lens was transferred to the spectrograph slit with the present lens/fiber-bundle optical system.

This fiber-optics-based light transfer system was used to avoid long-optical-path vibration effects and as a safety precaution because the instrumentation could then be placed in an area which was more remote and shielded from the immediate test environment.

Several other items were located on the spectrograph optical rail as shown in Figure 1 and the photograph in Figure 3. A removable mirror temporarily interrupted the optical path from the arc-heated flow. This mirror was used to direct the light from various calibration sources, also shown in Figure 3, onto the spectrometer entrance slit. A rotating mirror and condensing lens were used to select and focus radiation from either of the two calibrating sources. One such source was a Standard Lamp (STD Lamp in Figure 3). This was a tungsten ribbon lamp that had been calibrated against a similar lamp at the National Bureau of Standards. The

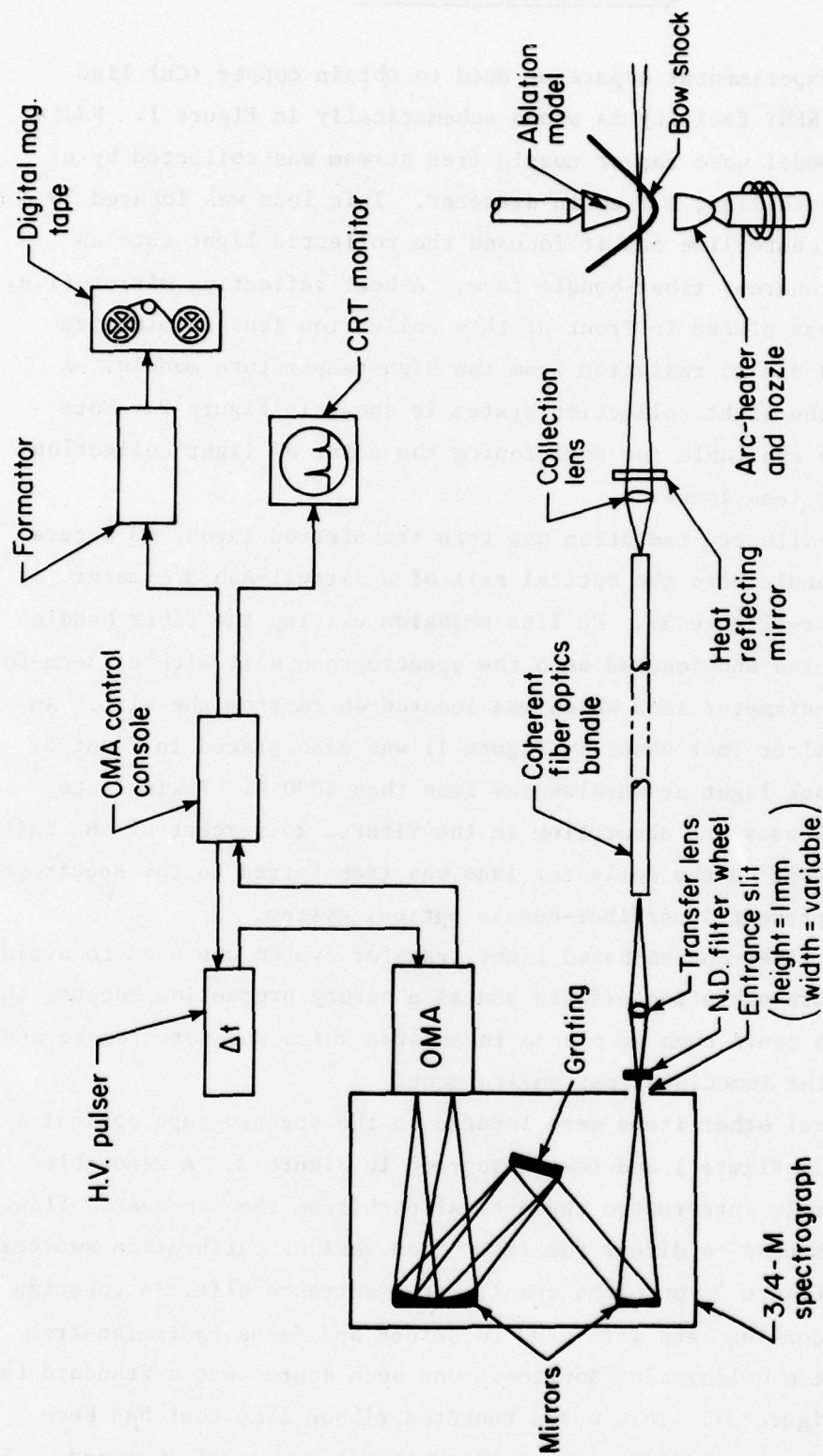


FIGURE 1. BLOCK DIAGRAM OF EXPERIMENTAL SETUP

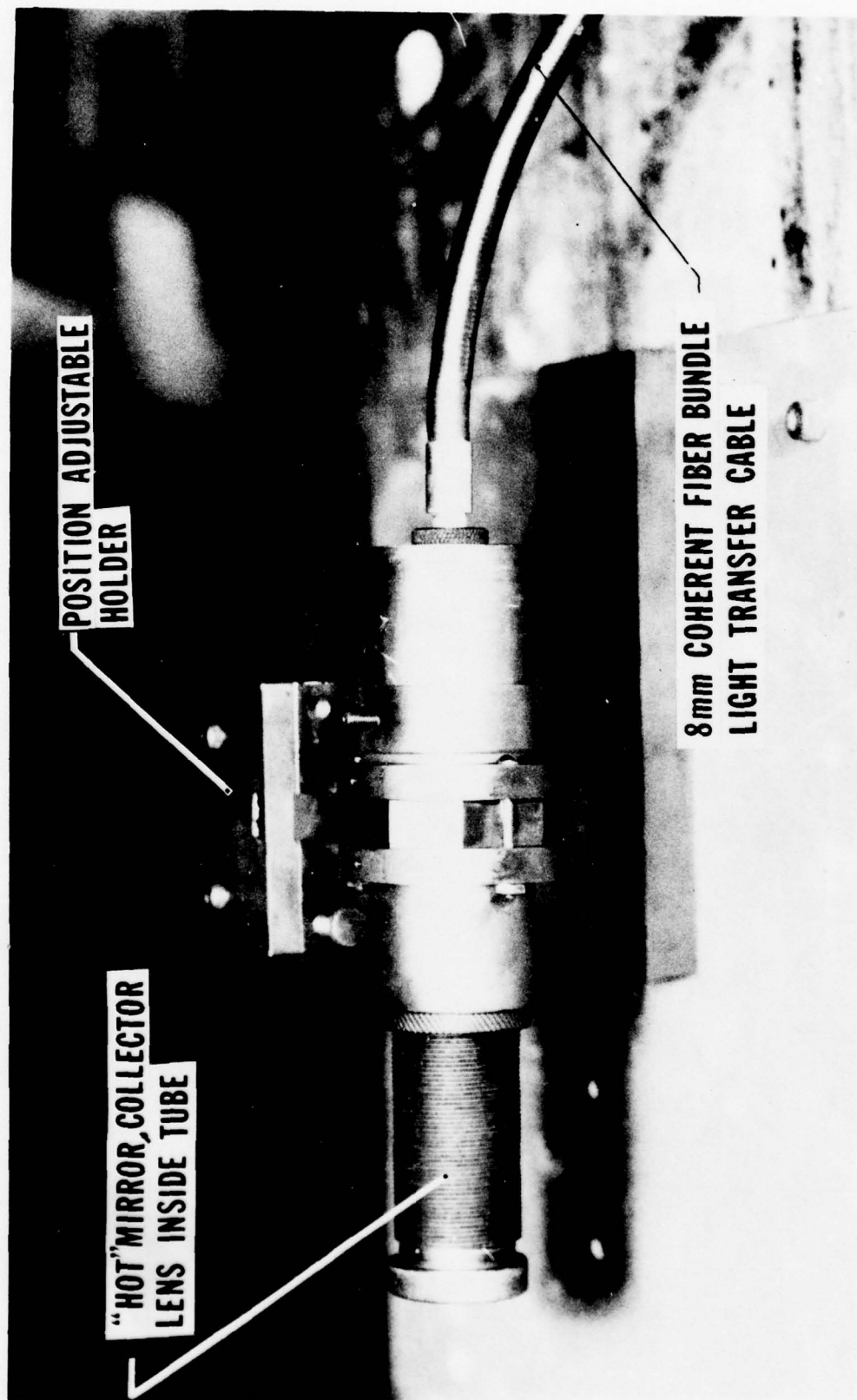


FIGURE 2. LIGHT COLLECTION AND TRANSFER SYSTEM

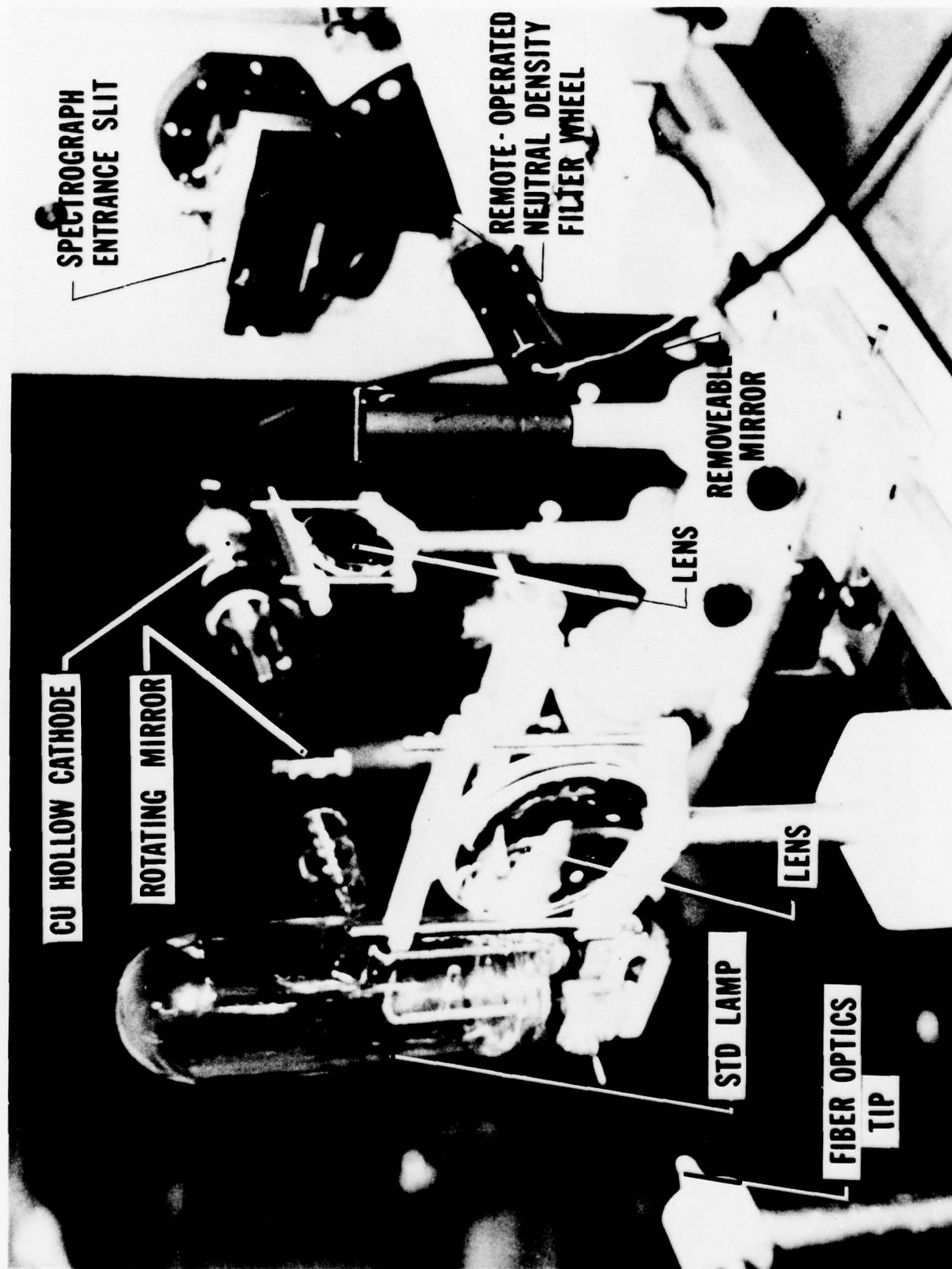


FIGURE 3. IMAGE TRANSFER AND CALIBRATION SYSTEM

absolute light output of the lamp at various wavelengths is published for a lamp current of 35 amperes. This lamp was used for a sensitivity calibration of the OMA detector screen. The other calibration lamp was a copper hollow-cathode lamp which was used to generate a known copper spectrum. This calibration spectrum was required in order to compute the $\text{\AA}/\text{channel}$ across the OMA screen for absolute line width measurements and to ascertain the spectral position of the copper lines prior to and after a tunnel run. This baseline position information was used to infer line shift information during the arc-tunnel tests.

Another piece of apparatus located on the spectrograph optical rail was a remotely operated, neutral-density filter wheel (see Figures 1 and 3). This device was used to provide variable attenuation of nose-cap radiation in case a detector was overloaded with incoming signal during early arc-tunnel runs.⁽⁵⁾

After passing through the spectrograph slit, the incoming radiation was collimated and diffracted using an 1180-grooves/mm grating in the first order. This grating was blazed at 7500 \AA . The spectrally analyzed radiation from the grating was then refocused onto the spectrograph exit plane (see Figure 1) using a larger camera mirror.

The OMA detector screen was located at this exit focal plane and was equivalent to placing 500 individual sensing elements (i.e., channels) 0.025 mm apart in a linear array across the exit plane of the spectrograph. Light incident on these sensing elements was converted to an electrical charge which was scanned off by a sweeping electron beam in a period of 32 msec . Several such time scans are required to completely erase this charge from the screen. In fact, 6-7 scans were used in this study so the time between successive data records was approximately 0.2 sec . Although this rather long time was required between data events, the actual data collection time (i.e., recording of the initial light intensities) was controlled with a high-voltage pulser that had a variable shutter time, Δt , down to as short as 50 nsec . In the present study, $10\text{-}100 \text{ }\mu\text{sec}$ shutter times were employed. Hence, the entire spectrum of the 5106 and 5153 \AA copper region was obtained simultaneously for a $10\text{-}100 \text{ }\mu\text{sec}$ period during the arc-tunnel run and at intervals of approximately 0.2 sec . This meant that three to ten spectral records per model were obtained depending on the model dwell time, which varied from 0.5 to 2 sec per model. Ten to

twenty free-stream data records were also obtained before the models were introduced. Then, four to five models were used for each arc-tunnel test so 12-50 model spectral line intensity records were obtainable at this data rate. For later arc-tunnel runs, the shutter time was remotely controlled during a run. Hence, the rotating neutral density filter wheel was no longer required for preventing detector overload. This feature provided for optimum light usage and quick change of OMA sensitivity when switching from free-stream to model data collection. Each data record was stored on a magnetic tape recorder for post-run data reduction.

Visual observation of the spectrum was also provided through the use of a CRT (Cathode Ray Tube) monitor, as shown in Figure 1. Furthermore, an audible OMA screen overload signal was supplied. Hence, by observing the CRT screen for weak signal indication and listening for the audible overload indicator, proper data acquisition could be obtained through operator adjustment of the remote shutter time (or neutral-density filter wheel) control.

III. ARC-FACILITY TESTING

A. Calibration

After installation, alteration, or substitution, of an OMA, the variation of output sensitivity across the screen was determined using the standard lamp system described above. The published lamp output was very nearly constant over the wavelength region encompassing the two copper lines of interest which simplified the determination of a sensitivity correction curve for use in the data reduction procedure. Output from each OMA channel was recorded and stored on magnetic tape. The sensitivity correction was then simply obtained from a ratio of the standard lamp output $I_{STD}(J)$ of each OMA channel, J , with the output of the particular channel, J_{PEAK} , that had the maximum output intensity, $I_{STD}(J_{PEAK})$. Hence, the correction factor, $C(J)$, was

$$C(J) = \frac{I_{STD}(J_{PEAK})}{I_{STD}(J)} \quad (1)$$

for $J = 1, 2, \dots, 500$

Raw copper line intensities from each data record that was stored on magnetic tape were corrected for screen sensitivity variation by multiplying each channel's apparent intensity, $I_A(J)$, by the above correction factor, such that

$$I_T(J) = I_A(J) \times C(J) \quad (2)$$

$J = 1, 2, \dots, 500$

where $I_T(J)$ is the true intensity of channel number J . Typical results for this sensitivity correction factor are shown in Figure 4 for two OMA screens used to record data reported herein. Note that a 50 percent correction must often be made near the edges of the screen but that the screen center region has a fairly flat response for both OMA's.

Prior to an arc-tunnel run, the OMA was temporarily removed and a flood lamp was placed at the exit plane of the spectrograph. This lamp provided a back light for the optical system such that an image of the

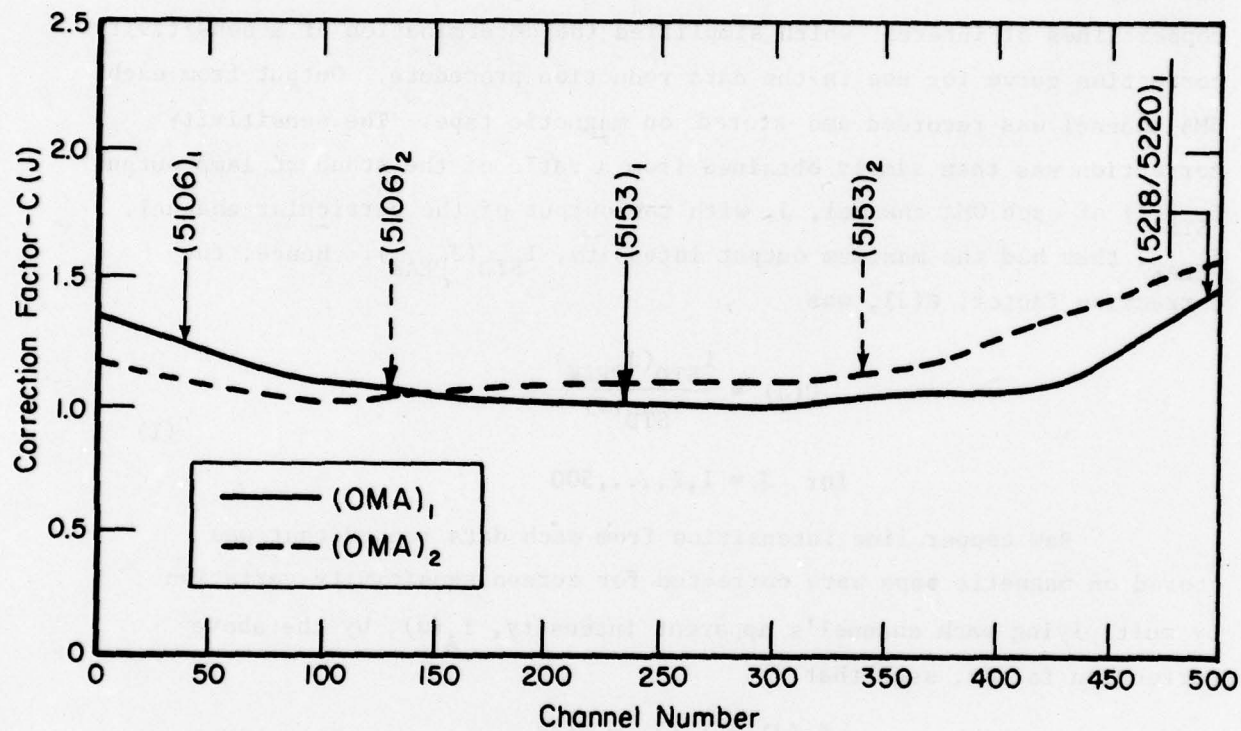


FIGURE 4. VARIATION IN SENSITIVITY ACROSS THE OPTICAL MULTICHANNEL ANALYZER (OMA) SCREEN FROM STANDARD LAMP CALIBRATION

entrance slit appeared at the tunnel exit plane. The image size was 1 mm long and, depending on the slit width, it was 0.05-0.1 mm wide. The image position and focus were then checked with respect to the tunnel axis. Image position was adjusted in order to center it on the nozzle axis at a position 1.27 mm (0.050 in.) downstream of the nozzle exit plane with the longest slit image dimension perpendicular to the nozzle axis. During a tunnel run, the models were held in position 2.54 mm (i.e., 0.10 in.) from the nozzle exit plane using a servo-positioning system driven by heat sensors pointed at the nose-tip material being ablated by the arc-heated gas flow. This arrangement put the slit image 1.27 mm off the receding graphite model nose-tip surface, between it and the detached bow shock wave.

Finally, several OMA spectral scans of the copper hollow-cathode lamp spectrum were stored on tape, just prior to the arc-tunnel run for wavelength calibration and line shift determination. The position of these lines on the OMA screen are also shown in Figure 4 for the various OMA types. Note that while using (OMA)₁, three lines were located on the screen; two near the edges and one near the centerline.⁽⁵⁾ However, when (OMA)₂ was utilized on later data taking sequences, the 5218/5220 doublet intensity was not recorded so that the 5106 and 5153 lines were located nearly symmetric about the screen centerline. The exact position (i.e., channel number) of these calibration lines was utilized in later data reduction procedures to provide an accurate measure of the number of wavelength units per OMA channel (i.e., Å/channel or plate factor) across the OMA screen. This information was required in order to convert line widths measured by the OMA into absolute wavelength units. Upon completion of this pre-run calibration, the removable mirror was extracted, thus preparing the diagnostic system for taking copper line intensity data during the actual arc-tunnel test.

A remote switch was used to initiate the acquisition of intermittent (i.e., approximately five times/sec) OMA data during the tunnel run. Post-run OMA data were also obtained using the Cu lamp source in order to check for the possibility of grating rotation due to vibration effects that accompanied the noisy arc-tunnel environment. End-of-file marks were automatically placed on the tape each time the remote switch was placed in the off position. This procedure provided a known separation between pre-run calibration, run data, and post-run calibration scans.

B. Preliminary Tests

After the Data Gathering System was installed in the RENT facility, preliminary data were obtained using the copper hollow lamp as a source during an actual in-house tunnel test (i.e., radiation from the tunnel flow was masked off). The purpose of these experiments was to ascertain what effects the electromagnetic and acoustic noise environments had on the data acquisition systems. It was found that the OMA output was affected by acoustic noise and its associated mechanical vibration.⁽⁵⁾ Direct mechanical vibration from water pumps and water flow also had a deleterious effect on OMA performance during a tunnel run. Vibration isolation of the spectrograph from its steel table stand was tried first using variable pressure vibration mounts. This direct isolation reduced but did not eliminate the interference. Next, an aluminum sheet metal enclosure was fabricated to cover the top and sides of the spectrograph and instrument rack. Lead vinyl sheet was attached to the inside of these aluminum enclosures and then foam pad was added to the vinyl sheet. Foam only was also attached to the plates on which the spectrograph and instrument rack were sitting. Hence, these instruments were completely surrounded by some acoustic material. Further, vibration isolation of the instrument rack was also accomplished using two layers of Isofoam rubber pad material sandwiched between aluminum plates between the instrument rack and the floor.

The above measures reduced the acoustic vibration interference on the OMA system to a negligible amount. They also reduced grating vibration which had affected line shift measurement accuracy. These system alterations enabled the continuation of copper line spectral analysis of arc-tunnel-induced radiation from the gas-cap and free-stream flow.

C. RENT Tests

Copper line intensity data were obtained from three high-swirl mode, arc-tunnel runs. Various types of graphite models and model dwell times were employed during these tests. The common tunnel conditions are listed in Table 1, and a partial test matrix is given in Table 2. The

TABLE 1. TUNNEL TEST CONDITIONS

Arc Current = 2600 amps

Arc Voltage = 9000 volts

Stagnation Pressure (p_o) = 100 atmospheres

09111P Nozzle: Throat Diameter = 0.9 inch
Exit Diameter = 1.11 inch

Nominal Mach No. = 1.8

Nominal Ratio of Specific Heats = 1.2

Nominal Exit Area Ratio = 1.52

TABLE 2. EXPERIMENTAL PARAMETERS FOR VARIOUS TUNNEL RUNS

Run Number	Date	Slit Width, μm	Model Dwell Time, sec	Shutter Time, μsec		OMA No.
				Free Stream	Models	
91-020	8/23/77	100	≈ 2.0	50	50*	1
91-029	3/10/78	50	≈ 0.6	70	20	2
91-030	3/13/78	50	≈ 0.6	90	20	2

* A neutral density filter with 20 percent transmission was used in this case to reduce light intensity in order to avoid sensing element overload.

shutter time and slit width listed in Table 2 refer to the OMA shutter and the spectrometer slit. Note that long model dwell times were available during Run No. 91-020. Air Force Materials Laboratory, high-quality, advanced graphite models were utilized on this test.⁽⁵⁾ All three models had a 1/2-inch (1.27-cm) nose diameter. For Run No. 91-020, free-stream data was obtained with a 50- μ sec shutter time with no neutral density, ND, filter attenuation. However, during the model data taking period, only 20 percent of the light could be utilized due to overload problems that occurred with the OMA detector. For the latter two runs (i.e., 91-029, 91-030), the variable shutter time feature was installed and the ND filter wheel was deactivated. Narrower slit widths were also utilized during the last two runs in order to obtain better line shape (i.e., width) and shift information.

During these latter runs, ATJ-S graphite, 1/2-inch-diameter flat-tipped models with phenol skirts were utilized. Severe ablation of the skirt material occurred during these tests with only modest material loss on the nose tip. Therefore, Runs 91-029 and 91-030 were restricted to short (i.e., ≈ 0.6 sec) model dwell times since damage to the model holding struts could have occurred if the skirt material failed. Note that a factor of 3-5 decrease in the shutter time was required between free-stream and model gas-cap data sequences to avoid overload problems.

IV. DATA REDUCTION PROCEDURE

A. General

OMA data from Runs 91-020, 91-029, and 91-030 were analyzed according to the procedure outlined in the Flow Chart of Figure 5. The nine-track digital tape recordings of the OMA data records were first decoded using a program that interpreted the tape and stored the data on a temporary file. Then, a data correction routine was used to correct the raw data for variations in gain across the OMA screen (see Figure 4). Example plots of corrected data scans for calibration and model gas-cap conditions are shown in Figure 6 for Run No. 91-020. Note the presence of three major lines in the arc-tunnel spectrum which are easily identified from the corresponding calibration scan. However, only the 5106 and 5153 Å lines were used in the following data analysis procedure. Note also the continuum background radiation present in the spectral scan from the model gas-cap emission.

Several tests were then performed on the corrected spectral data to ascertain if the data were acceptable for analysis. These tests comprised:

- (1) A check for weak or no signal above the background level (i.e., poor line-signal-to-background-signal ratio).
- (2) A check for overload (i.e., peak line signal larger than linear range of OMA screen).

If the signal failed either of these tests, the data for that particular OMA record was stored on a rejected data tape along with its identification number and a diagnostic message identifier. If the signal passed the above tests, it was analyzed with a Gaussian curve-fit routine which determined the best least-squares fit of the spectral line intensity data. Outputs of this Gaussian curve-fit subroutine included:

- Channel number of the line peak intensity point, J (note: fractions-of-a-channel numbers are permissible)

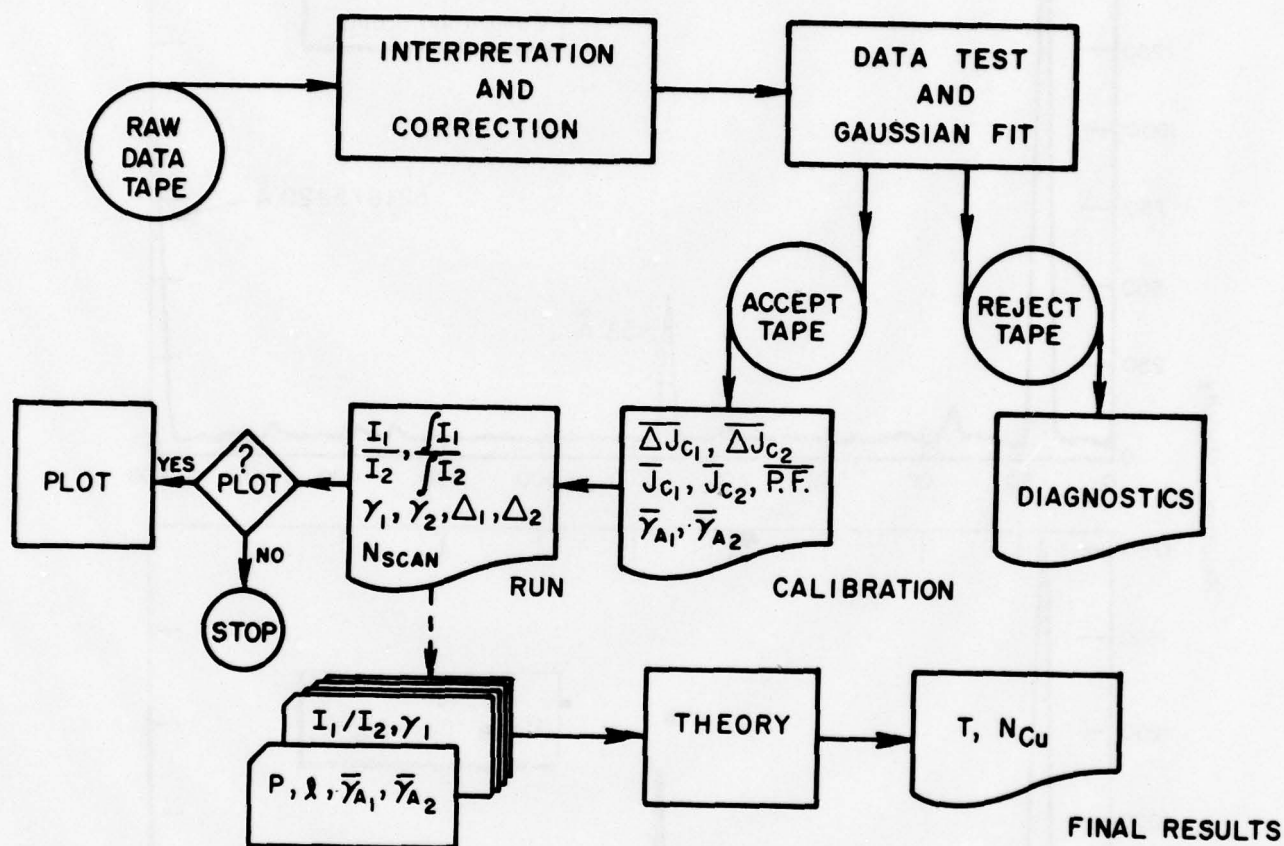


FIGURE 5. FLOW CHART DESCRIBING DATA REDUCTION PROCEDURE FOR OBTAINING TEMPERATURE AND COPPER DENSITY FROM THE RAW SPECTRAL MEASUREMENTS

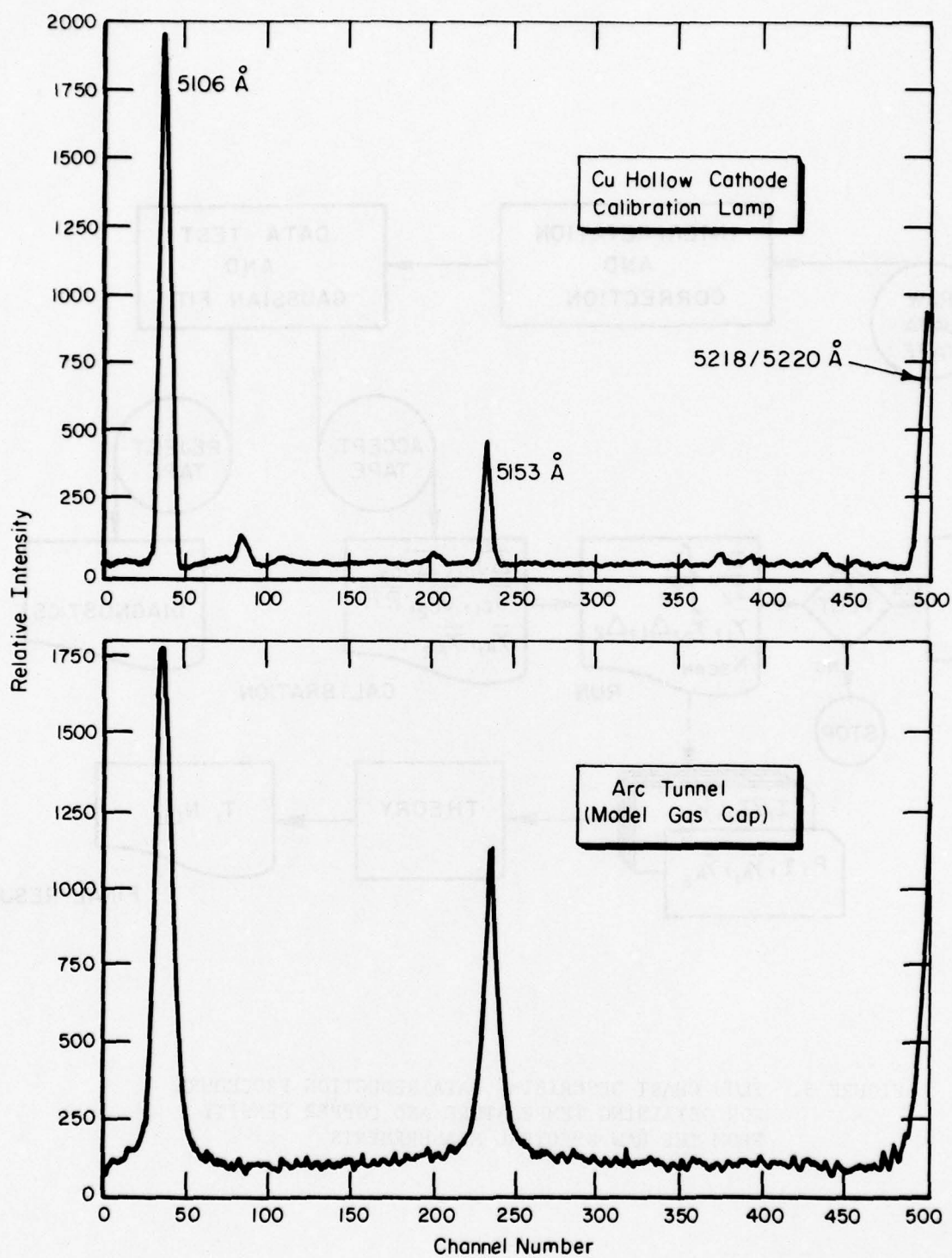


FIGURE 6. OPTICAL MULTICHANNEL ANALYZER (OMA) SCANS FOR CALIBRATION AND TEST CONDITIONS (RUN NO. 91-020)

- Value of the line peak intensity above the background, I
- Value of the background intensity in the immediate region of the line
- Full width of the line at one-half the peak line intensity value in channel numbers, ΔJ (again fractions of channel numbers are permissible)
- Value of the integrated intensity of the line determined from a numerical integration of the intensity values above the background level using Simpson's rule, $\int I$.

These output values for both lines of a particular data scan were then stored on a tape labeled Accept Tape in Figure 5. Occasionally, the Gaussian fit subroutine would not converge in a prescribed number of iterations. If this occurred, the scan data were stored on the reject tape with the appropriate diagnostic identifier.

The accept and reject tapes were then further analyzed to obtain usable line shape and shift information. The reject tape was simply printed to indicate which line scans failed to be analyzed and for what reasons. The accept tape was analyzed in the order of the appearance of data on the tape itself. Pre-run calibration data were always stored first so these data were analyzed first to provide the following outputs:

- The average channel number \bar{J}_{c_1} and \bar{J}_{c_2} for each of the two calibration line peak intensity positions from 10-15 data scans. The subscripts 1 and 2 refer to the 5106 and 5153 Å lines, respectively.
- Average width of the two calibration lines in channel numbers (i.e., $\Delta \bar{J}_{c_1}$, $\Delta \bar{J}_{c_2}$). This width was taken to be that of the apparatus functions.

Note that all of the above values could be fractions of channel numbers. From the difference in the average positions of the two copper calibration lines on the OMA screen and the known separation of these lines (i.e., $5153.24 - 5105.54 = 47.70$ Å), the average plate factor, $\overline{P.F.}$, for the OMA screen was automatically determined using the following:

$$\overline{P.F.} = \frac{47.70}{(\overline{J}_{c_2} - \overline{J}_{c_1})} \quad [\text{\AA}/\text{Channel}] \quad . \quad (3)$$

This plate factor was then used to convert the calibration line widths (i.e., apparatus function widths) into angstrom units using the following:

$$\left. \begin{aligned} \overline{\gamma}_{A_1} &= \overline{P.F.} \quad \overline{\Delta J}_{c_1} \\ \overline{\gamma}_{A_2} &= \overline{P.F.} \quad \overline{\Delta J}_{c_2} \end{aligned} \right\} \quad [\text{\AA}] \quad . \quad (4)$$

Example plots of the raw calibration data and resultant Gaussian fits are shown in Figures 7a and 8a for a 0.050-mm entrance slit. Note that the widths of the two calibration lines (i.e., apparatus function widths) differ by 0.15 Å for this particular data record due to focus variations across the OMA screen. An average of the widths of 15 such data records gives:

$$\begin{aligned} \overline{\gamma}_{A_1} &= 0.98 \pm 0.02 \text{ \AA} \\ \overline{\gamma}_{A_2} &= 0.80 \pm 0.04 \text{ \AA} \end{aligned} \quad . \quad (5)$$

These latter apparatus width values were subsequently utilized in the data reduction procedure to convert spectral data into final temperature and copper density results for Runs 91-029 and 91-030.

After the calibration data were analyzed, the next block of data on the accept tape (i.e., run data) was processed using results determined during the calibration analysis procedure. The plate factor was used to convert the Gaussian-fit line widths ΔJ_1 and ΔJ_2 from the arc-tunnel flow emission data into wavelength equivalents (i.e., γ_1 and γ_2) using

$$\left. \begin{aligned} \gamma_1 &= \overline{P.F.} \quad \Delta J_1 \\ \gamma_2 &= \overline{P.F.} \quad \Delta J_2 \end{aligned} \right\} \quad [\text{\AA}] \quad . \quad (6)$$

Line shift values were also automatically determined from the run data by using the average position information results from the calibration analysis. Thus, the line shift, Δ , relative to the calibration value was determined using the following:

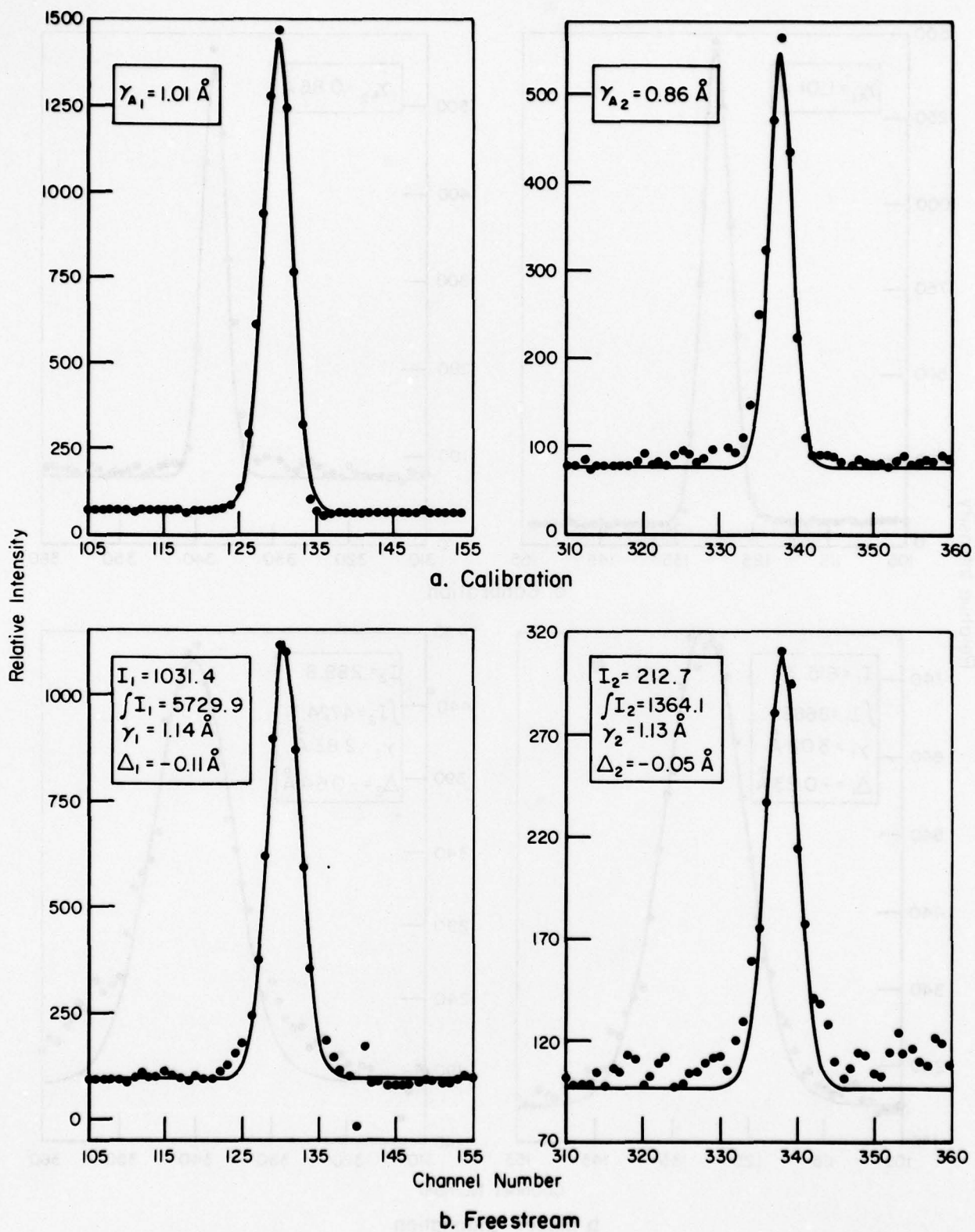


FIGURE 7. OMA DATA RECORDS FOR CALIBRATION AND FREE-STREAM CONDITIONS DURING RUN NO. 91-029

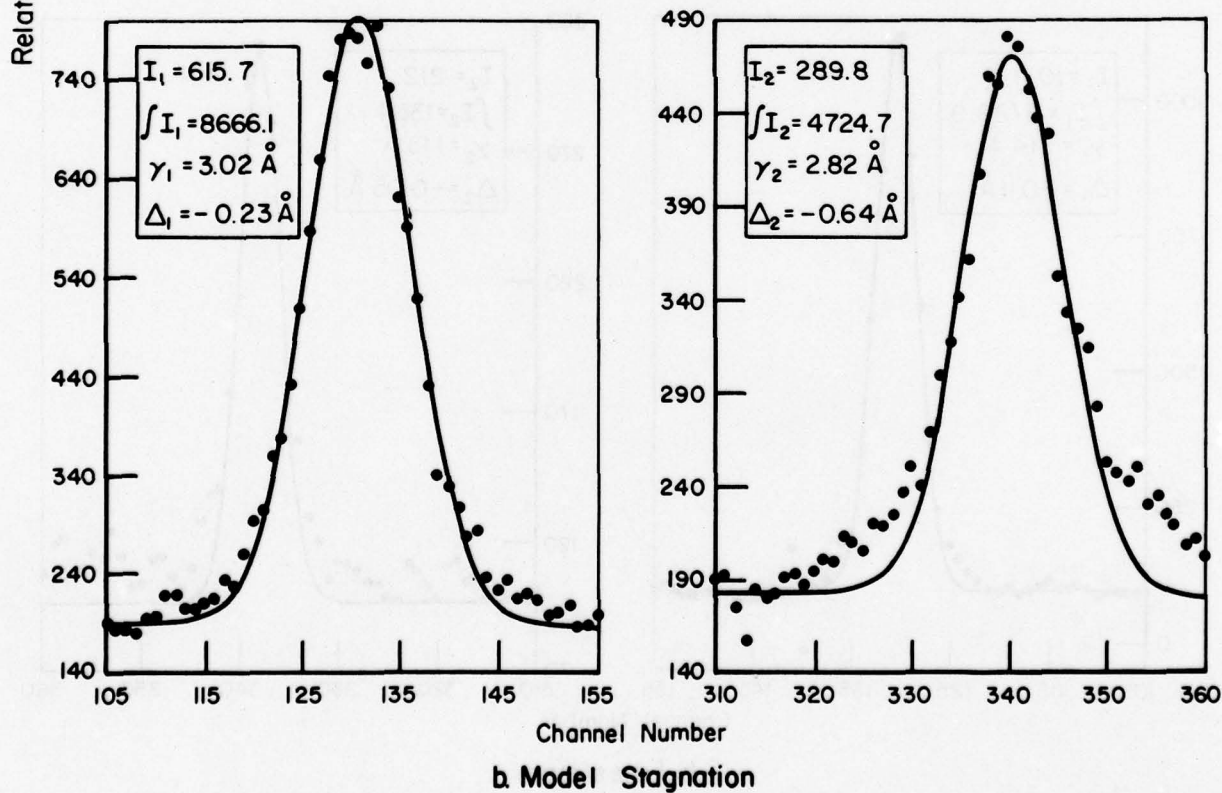
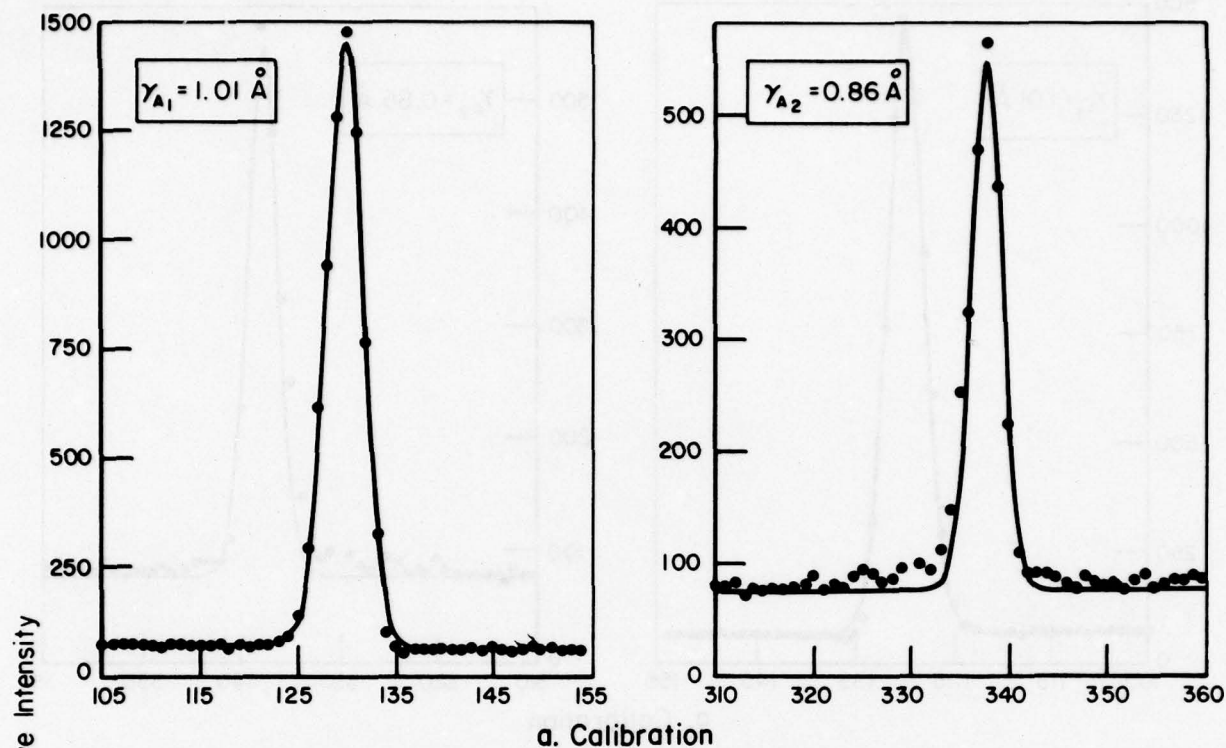


FIGURE 8. OMA DATA RECORDS FOR CALIBRATION AND MODEL GAS-CAP CONDITIONS DURING RUN NO. 91-029

$$\begin{aligned}\Delta_1 &= (\bar{J}_{c_1} - J_1) \overline{P.F.} \\ \Delta_2 &= (\bar{J}_{c_2} - J_2) \overline{P.F.}\end{aligned}\quad \begin{matrix} [\text{\AA}] \\ (7) \end{matrix}$$

where J_1 and J_2 are the positions (i.e., channel numbers of the line peaks) for the lines during the particular run scan. Note that in Equation (7) a shift to longer (i.e., red wavelengths, $J_i > \bar{J}_{c_i}$) will result in a negative value for Δ .

Ratios of the peak intensities of the two lines, I_1/I_2 , and the integrated line intensity ratio (i.e., $\int I_1/\int I_2$) were also determined automatically; and all this information was printed for each acceptable data scan during the arc-tunnel run. Typical results of this arc-tunnel data analysis procedure are shown listed in Figures 7b and 8b for free-stream and model gas-cap conditions during Run No. 91-029. In Figure 7b, an OMA data record of the 5106 and 5153 line spectrum for free-stream conditions (i.e., no models) shows that any line broadening which occurred was much less than the apparatus function width.

However, spectral data obtained from the model stagnation region which is shown in Figure 8b indicates that the increased width is three times the apparatus function width. Gaussian curve fits to the above OMA data are also shown in these figures. Note that the Gaussian fit provides quite accurate values for the width and peak intensity of the copper emission lines of interest for typical arc-tunnel conditions. The increased magnitude of line width and red shift can also be seen in Figure 8b for the model stagnation case over the free-stream condition. This is due to the fact that the number of broadening collisions increases because of the gas density increase across the bow shock wave.

B. Theory for Self-Absorption Corrections

Before temperature and number density could be obtained from the measured line width and intensity data shown in Figures 7b and 8b, copper line intensity and line shape had to be calculated as a function of gas temperature, T , and copper density, N_{Cu} . The details of this theoretical procedure will not be presented here. It suffices to say that a theory which is normally attributed to Lindholm⁽⁷⁾ was available to predict line

intensity and shape for the above variables provided certain basic atomic constants are known. The theory for integrated line intensity ratio was coded into a digital computer program by AFFDL personnel in previous work.⁽⁴⁾ This code was modified during the present study to include the determination of line shape and peak line intensity as a function of temperature and copper density.⁽⁸⁾ For details concerning the theory and associated atomic constants, the reader should consult References 6-9.

The code first calculated the true line shape (i.e., infinitely narrow instrument apparatus function) and plotted the results of this calculation. However, since most spectral data are obtained with a finite slit width, some convolution will occur between the true and measured line shape in actual practice. Therefore, the code also included the possibility of inputting a Gaussian-shaped instrument apparatus function with a full half-width, $\bar{\gamma}_A$, as a code input parameter. The convoluted line profile was then calculated and also plotted. The half-width and peak intensity of the true and convoluted line as well as the integrated line intensity are also calculated by the code and printed out on the line shape plot.

Some basic program inputs are the gas pressure, p , and the length of the radiating gas region, ℓ . For the present analysis, $p = 80$ atm and $\ell = 2.0$ cm (0.8 inch) were used for the model gas-cap calculations and $p = 19$ atm, $\ell = 1$ cm (0.4 inch) were assumed for the free-stream case.

The above nominal pressures were determined in previous measurements by AFFDL personnel using a swept copper pitot probe. The dimensions of the radiating gas regimes (i.e., ℓ 's) were obtained from photographs of the high-temperature flow. In the model stagnation case, a photograph of the radiating gas behind a bow shock wave on a typical model was utilized to determine the required characteristic length. This length (i.e., $\ell = 2$ cm) was 37 percent greater than the model nose diameter of 0.5 inch (i.e., 1.27 cm). For the free-stream case, a photograph of the nozzle exit flow indicated a small bright region in the flow which corresponds to the characteristic spike in the nozzle exit heat flux profile. Estimates are that this region is approximately 0.4 inch (i.e., $\ell \approx 1$ cm) in length. Therefore, the length of this dominant radiation region was utilized as the characteristic length of the free-stream flow even though the total physical extent of the free-stream itself exceeded approximately 3 cm (1.2 inch).

Several assumptions were required for applying the copper line intensity theory given in Reference 8, namely:

- Temperature and copper density spatial uniformity in the emission region defined by ℓ
- Radiatively inactive free stream for gas-cap measurements
- Local thermodynamic equilibrium (LTE)
- Pressure is constant.

A further assumption of an optically thin gas was not needed since the theory accounted for variations in copper density. This latter assumption is required for the simple line ratio measurement of temperature where self-absorption of copper radiation by other copper atoms is assumed negligible. However, when self-absorption does occur, the copper density must also be measured and the optically thin temperature corrected for self-absorption effects. This correction was accomplished, in the present case, by simultaneously measuring the full half-width of the 5106 Å copper line along with the line intensity ratio (see Reference 8).

Results of the theoretical computation for peak intensity ratio and 5106 Å line width as a function of temperature and copper density are shown in Figure 9 for model gas-cap environment. This figure would have to be replotted for any change in run conditions that involved a change in ℓ , p , $\bar{\gamma}_{A1}$, or $\bar{\gamma}_{A2}$. The instrument apparatus functions, $\bar{\gamma}_A$'s, used in the code calculation shown in Figure 9 were taken from results of the copper calibration lamp spectrum analysis above [see Equation (5)].

The curves in Figure 9 could be utilized directly to reduce spectroscopic data taken with the same apparatus function. However, a cumbersome iteration process would be required whereby measured values of intensity ratio and 5106 Å line width are used to locate a set of temperature and copper density values that are consistent with both of these measured parameters. A simpler way to reduce the data was obtained with crossplots constructed from the theory plots in Figure 9. These crossplots were obtained by picking constant values of intensity ratio and line width and finding the points of intersection of these values with the constant temperature and copper density curves in Figure 9. New curves were then constructed with temperature and density for the variables as shown in Figure 10.

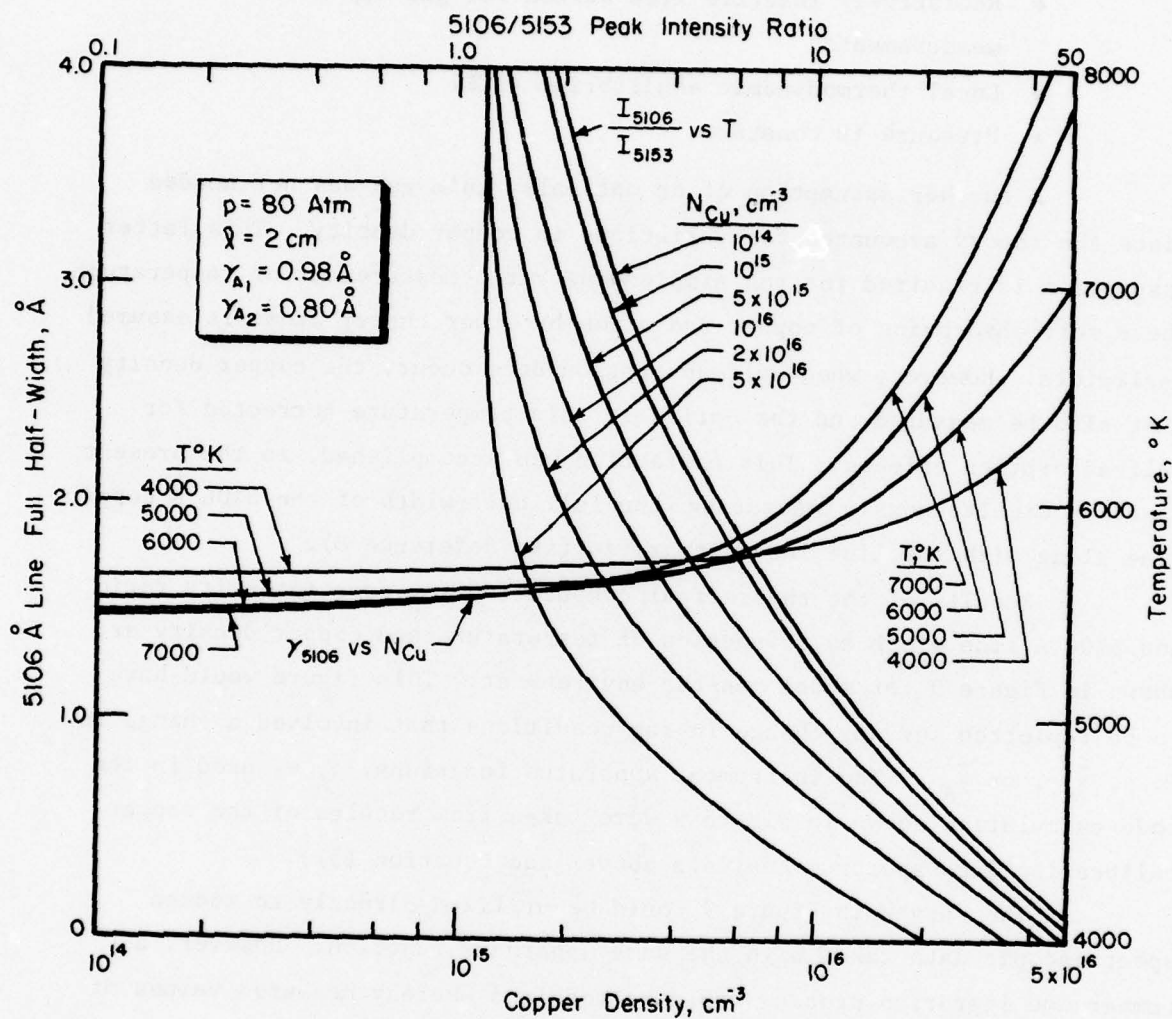


FIGURE 9. ACTUAL THEORETICAL 5106 TO 5153 Å LINE INTENSITY RATIO AND 5106 Å LINE FULL-WIDTH AS A FUNCTION OF TEMPERATURE AND COPPER DENSITY FOR CONDITIONS OF RUN NO. 91-029 AND 91-030 ($p = 80 \text{ atm}$, $l = 2 \text{ cm}$, $\gamma_A = 0.98 \text{ Å}$, $\gamma_{A2} = 0.80 \text{ Å}$)

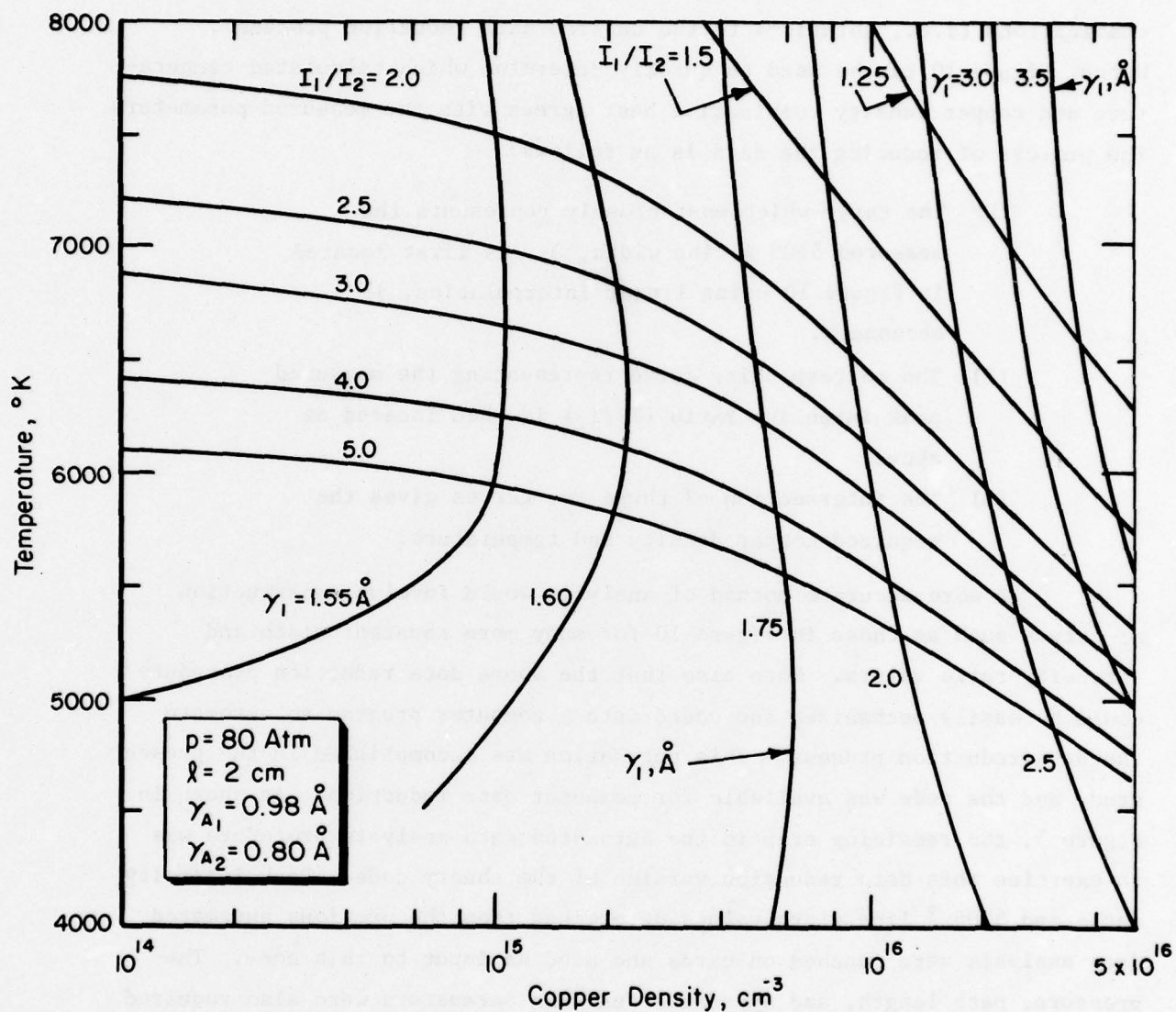


FIGURE 10. THEORETICAL CURVES USED TO REDUCE MEASURED LINE INTENSITY RATIO AND LINE WIDTH DATA IN ORDER TO OBTAIN SIMULTANEOUS TEMPERATURE AND COPPER DENSITY RESULTS FOR RUN NO. 91-029 AND 91-030 ($p = 80 \text{ atm}$, $l = 2 \text{ cm}$, $\gamma_{A_1} = 0.98 \text{ \AA}$, $\gamma_{A_2} = 0.80 \text{ \AA}$)

In Figure 10, the importance of knowing the copper density is evident if accurate temperature is to be inferred from line intensity ratio data. Note that only for optically thin conditions is the line intensity ratio independent of flow copper density. The intersection of the two families of curves in Figure 10 defines compatible temperature copper density combinations (i.e., solutions to the desired data reduction process). Hence, Figure 10 can be used to quickly determine which calculated temperature and copper density combination best agrees with the measured parameters. The process of reducing the data is as follows:

- (1) The curve which most closely represents the measured 5106 Å line width, γ_1 , is first located in Figure 10 using linear interpolation, if necessary.
- (2) The corresponding curve representing the measured peak intensity ratio (I_1/I_2) is then located as above.
- (3) The intersection of these two curves gives the required copper density and temperature.

A more accurate method of analysis would involve construction of curves such as those in Figure 10 for many more constant width and intensity ratio values. Note also that the above data reduction procedure could be easily mechanized and coded into a computer program to automate the data reduction process. This automation was accomplished in the present study and the code was available for computer data reduction. As shown in Figure 5, the remaining step in the automated data analysis procedure was to exercise this data reduction version of the theory code. Peak intensity ratio and 5106 Å line width values determined from the previous automated data analysis were punched on cards and used as input to this code. The pressure, path length, and apparatus function parameters were also required as shown in Figure 5. The code output provided the final temperature and copper density results required to define the arc-tunnel flow enthalpy, including self-absorption effects.

C. Example Calculations

To see how the curves of Figures 9 and 10 are used to infer gas-cap temperature and copper density for Run No. 91-029, an example calculation was performed using the data in Figure 8b. Note from this figure that

$$\begin{aligned}\frac{I_1}{I_2} &= 2.12 \\ \gamma_1 &= 3.02 \text{ \AA}\end{aligned}\tag{8}$$

Taking the value of 2.12 for the ratio of peak intensities, and using the $N_{\text{Cu}} = 10^{14}$ curve (i.e., optically thin) in Figure 9, the optically thin temperature can be found directly. Hence,

$$T_{\text{opt thin}} = 7580 \text{ K}\tag{9}$$

However, using Figure 10, it is evident that for a line width near 3 Å and a ratio near 2, the copper density is approximately 5×10^{16} Atoms/cm³ or 500 times the optically thin limit. It is also obvious from Figure 10 that the temperature is actually closer to 5400 K which is much less than the optically thin value given in Equation (9). More accurate computer calculations show that the temperature, T , and copper density, N_{Cu} , including self-absorption are

$$\begin{aligned}T &= 5410 \text{ K} \\ N_{\text{Cu}} &= 4.0 \times 10^{16} \text{ Atoms/cm}^3\end{aligned}\tag{10}$$

This example points out the importance of correcting the simple line ratio temperature measurement for self-absorption effects.

V. EXPERIMENTAL RESULTS AND DISCUSSION

A. Temperature and Enthalpy

The data reduction procedure outlined in Section IV was performed for all the pertinent calibration and run data. The resultant optically thin temperatures and temperatures corrected for self-absorption effects are plotted in Figure 11 as a function of tunnel run time following the first model injection. The presence of a model in the flow is also indicated using time bars in Figure 11.

In Figure 11a (i.e., Run No. 91-020), the data for Models 1 and 2 were sparse due to the fact that adjustments had to be made for the value of the neutral-density filter in front of the entrance slit because several overflow conditions occurred during these model dwell times. Once proper adjustments were made, more useful data were obtained for Models 3 and 4. Model data for Runs 91-029 and 91-030 (i.e., Figures 11b and 11c) were also sparse but, in this case, the short model dwell time was the cause. Free-stream data during Run No. 91-020 were not usable for obtaining temperature results corrected for self-absorption effects due to the broad apparatus function used during this test sequence (i.e., 100- μ m slit--see Table 2). However, the average optically thin free-stream temperature was determined to be 5440 ± 400 K for Run No. 91-020. This value, which is not shown in Figure 11, is in good agreement with the overall average free-stream optically thin temperature of 5720 K, which was determined from the other tunnel runs.

Large (i.e., 10-20 percent) fluctuations in temperature can be noted in Figure 11. The cause of these fluctuations is not known at this time but may be due to a variety of sources associated with the arc itself. These fluctuations are expected to be less for the constricted arc facility being developed at AFFDL. Also note that the fluctuations seem larger for Runs 91-029 and 91-030. This could be due to the fact that a factor of 2.5 times shorter data acquisition time was utilized on these latter tests (see Table 2) which resulted in less temporal smoothing of the copper line emission data. Finally, Figure 11 shows that a larger factor is required to correct the optically thin data for self-absorption effects in the latter

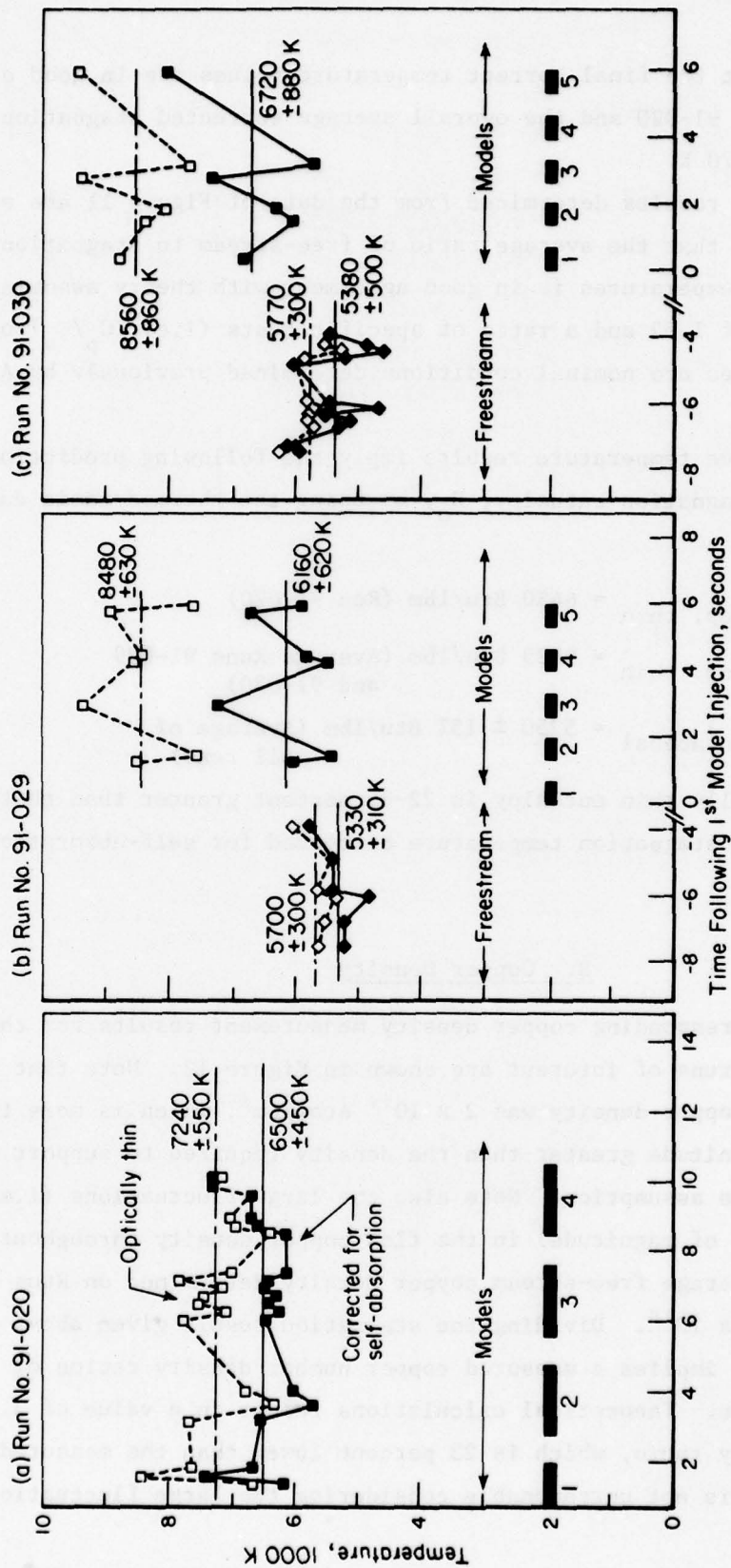


FIGURE 11. FREE-STREAM AND MODEL STAGNATION TEMPERATURE RESULTS FOR VARIOUS ARC-TUNNEL RUNS

two runs, but that the final correct temperature values are in good agreement with Run No. 91-020 and the overall average corrected stagnation temperature of 6470 K.

Further results determined from the data of Figure 11 are shown in Table 3. Note that the average ratio of free-stream to stagnation (i.e., gas-cap) temperatures is in good agreement with theory assuming an exit area ratio of 1.52 and a ratio of specific heats (i.e., C_p/C_v) of 1.2. These latter values are nominal conditions determined previously by AFFDL personnel.

The above temperature results imply the following prediction of the average stagnation enthalpy, H_o , by using the thermodynamic data in Reference 10.

$$\begin{aligned} (H_o)_{\text{op. thin}} &= 6450 \text{ Btu/lbm (Run 91-020)} \\ (H_o)_{\text{op. thin}} &= 9825 \text{ Btu/lbm (Average Runs 91-029 and 91-030)} \\ (H_o)_{\text{actual}} &= 5250 \pm 15\% \text{ Btu/lbm (Average of all runs)} \end{aligned} \quad (11)$$

Hence, the optically thin enthalpy is 22-85 percent greater than that determined from a stagnation temperature corrected for self-absorption effects.

B. Copper Density

The corresponding copper density measurement results for the given arc-tunnel runs of interest are shown in Figure 12. Note that the average gas-cap copper density was 2×10^{16} Atom/cm³, which is more than two orders of magnitude greater than the density required to support the optically thin gas assumption. Note also the large fluctuations (i.e., one to two orders of magnitude) in the flow copper density throughout the run time. The average free-stream copper density determined on Runs 91-029 and 91-030 was 5×10^{15} . Dividing the stagnation result given above by this free-stream value implies a measured copper number density ratio of 4 across the bow shock wave. Theoretical calculations result in a value of 3.25 for the number density ratio, which is 23 percent lower than the measured value. This discrepancy is not unreasonable considering the large fluctuations

TABLE 3. AVERAGE FREE-STREAM AND MODEL GAS-CAP TEMPERATURE RESULTS FROM ALL TUNNEL DATA COMPARED TO THEORY FOR PRESENT NOZZLE FLOW CONDITIONS

$\bar{T}_{FS},$ °K	$\bar{T}_O,$ °K	\bar{T}_{FS}/\bar{T}_O (exp)	T_{FS}/T_O (Theory)
5360 ±440	6470 ±590	0.83* (+9%)	0.76**

* T_{FS}/T_O (opt. thin) = 0.67 from Runs 91-029 and 91-030, which is 11 percent too low.

** Assumes $A/A_* = 1.52$, $\frac{C_p}{C_v} = 1.2$ (see Table 1).

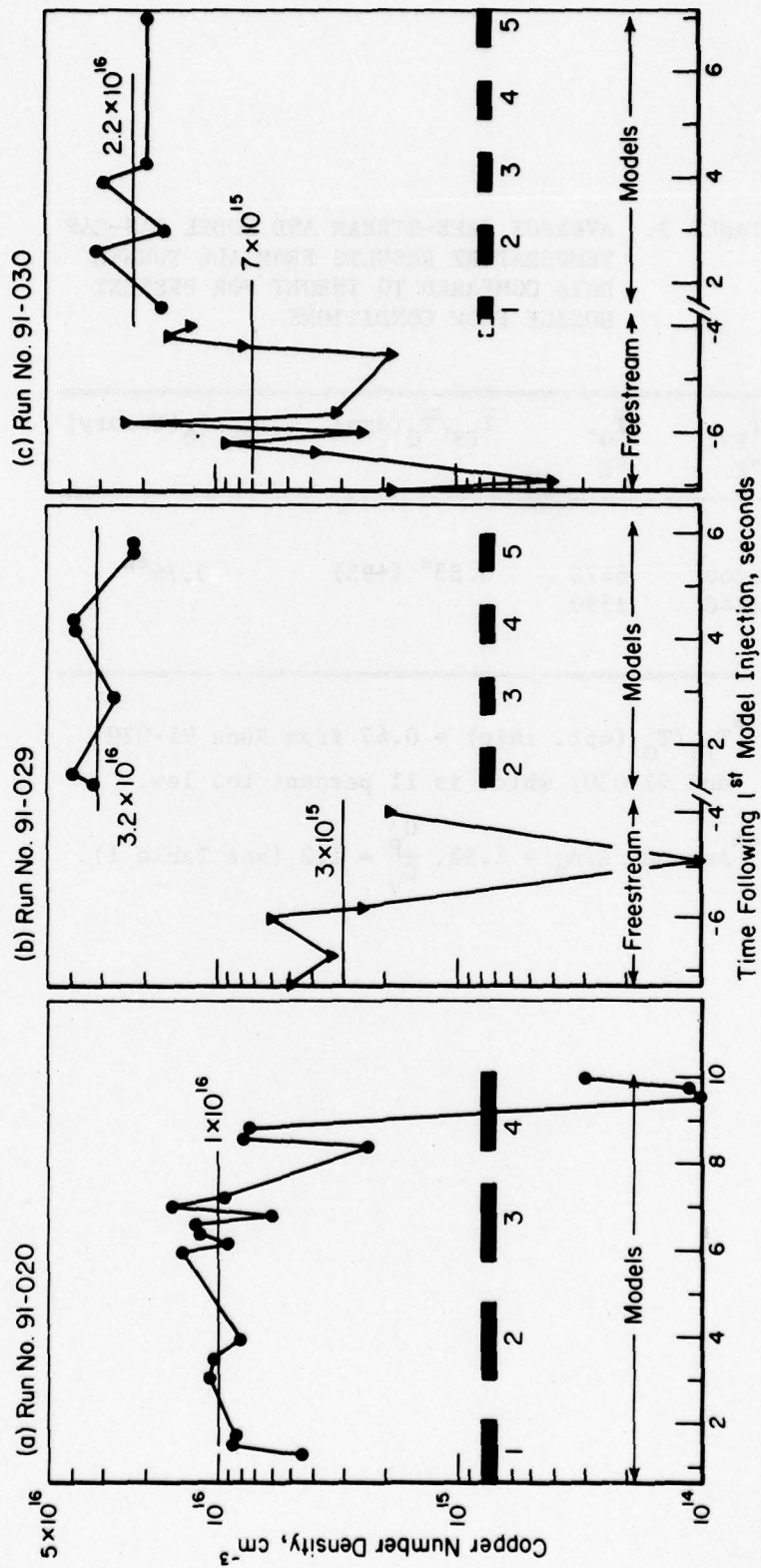


FIGURE 12. COPPER DENSITY DATA OBTAINED FOR FREE-STREAM AND MODEL STAGNATION CONDITIONS DURING SEVERAL ARC-TUNNEL RUNS

in the measured values which make it difficult to define a mean value in the first place, and the approximations involved in predicting an accurate optical path length, ℓ , for the free-stream environment.

C. Free-Stream Radiation

Free-stream flow in the RENT facility operating in the "high swirl" mode is characterized by a local "hot" zone near the center of the flow and a region of cooler gas surrounding this hot core.⁽¹¹⁾ The free-stream temperature measurements given above were assumed to be indicative of this "hot" core region of the flow. The "cold" flow zone was assumed to be radiatively inactive (i.e., no emission contribution and no absorption of "hot" zone copper line radiation). Measurements of stagnation point heat flux across the nozzle exit plane indicated that the temperature of this "hot" core was 80 percent higher than the surrounding "cold" flow region.⁽¹¹⁾

When a model is placed into the flow field, the "hot" core impinges upon the stagnation region between the blunt model and the bow shock wave and the cooler free-stream gas flows around this shock-heated region. It was also assumed in the analysis of the gas-cap copper line radiation data given above that the "cold" free-stream flow could be considered radiatively inactive with respect to these stagnation point measurements. This is equivalent to assuming that copper line radiation emanating from the stagnation zone of a model in the flow field is negligibly affected by the "cold" free-stream flow between the gas cap and the light collection lens (i.e., no emission or absorption contribution to the overall line spectrum). In this section, the validity of the above radiation inactivity assumptions is examined in some detail.

Theoretical formulations given in Reference 8 indicate that the peak intensity of the 5106 and 5153 Å lines for optically thin conditions can be approximated by the following equations:

$$\left. \begin{array}{l} I_{5106} \propto N_{\text{Cu}} \ell T^3 \\ I_{5153} \propto N_{\text{Cu}} \ell T^9 \\ \text{or } I_{5153}/I_{5106} \propto T^6 \end{array} \right\} \begin{array}{l} \text{(optically thin)} \\ \end{array} \quad (12)$$

for $3500 < T < 6500 \text{ K}$.

Equation (12) can, therefore, be used to estimate the copper line intensities for various optically thin flow conditions.

Between the model gas cap and the "hot" core of the free-stream, the measured copper density was a factor of 4 higher for the gas cap, and the length of the radiating region, ℓ , was a factor of 2 larger. Furthermore, the measured temperature was 20 percent greater for the stagnation flow over that of the "hot" free stream. Therefore, Equation (12) would predict a factor of 14 [i.e., $4 \times 2 \times (1.2)^3$] larger 5106 Å line intensity for the gas-cap flow over the "hot" free-stream region. Present measurements indicated that a factor of 3-5 intensity variation actually existed between these two flow regions.

Equation (12) could also be used to predict the variation of the 5153 Å line intensity for these flow conditions. In this case, a factor of 41 [i.e., $4 \times 2 \times (1.2)^9$] was calculated. However, a 9-12 intensity ratio between model and "hot" free stream was actually obtained in the present study. The above intensity ratio discrepancies are due to the fact that self-absorption of copper line radiation occurred for the gas-cap environment, so the optically thin assumption required for application of Equation (12) was violated in this case.

For the free-stream, however, the copper density and temperature measurements (i.e., sections V-A and V-B) indicated that this flow environment was nearly optically thin, so Equation (12) can be utilized with greater accuracy for free-stream intensity variation calculations. In this case, the copper density was assumed constant across the nozzle exit plane, but the path lengths of the "hot" and "cold" zones were unequal ($\ell = 1$ cm for "hot" zone and $\ell = 2$ cm for "cold" region). The temperature ratio between "hot" and "cold" regions was taken to be 1.8, as given above. Hence, the intensity ratio of the various lines can be written as

$$\left. \begin{aligned} \left(\frac{I_{\text{hot}}}{I_{\text{cold}}}_{5106} \right) &\cong \frac{1}{2}(1.8)^3 = 3 \\ \left(\frac{I_{\text{hot}}}{I_{\text{cold}}}_{5153} \right) &\cong \frac{1}{2}(1.8)^9 = 100 \end{aligned} \right\} \quad (13)$$

Combining these calculated variations between the "hot" and "cold" regions of the free stream with the measured intensity ratios between the model stagnation zone and the "hot" free-stream core region, we finally obtain

$$\frac{I_{\text{stagnation}}}{I_{\text{"cold" free stream 5106}}} \approx 12 \quad (14)$$

$$\frac{I_{\text{stagnation}}}{I_{\text{"cold" free stream 5153}}} \approx 1000 .$$

The results given in Equation (14) indicate that, for the stagnation flow copper line measurements, the "cold" free stream contributes negligibly to the overall peak line radiation intensity. Hence, for this case, the free-stream flow can be considered radiatively inactive (i.e., second assumption in Section IV-B is valid). However, in the case of free-stream copper line measurements, Equation (13) implies that, for a constant copper density across the flow, some problems may exist for obtaining accurate free-stream results. In this case, the 5153 Å line intensity profile would be representative of the "hot" zone conditions only, while the 5106 Å line profile would be indicative of a combination of the "hot" and "cold" zone environments since approximately 25 percent of the observed 5106 Å line intensity originates from the "cold" flow zone. This is equivalent to saying that the conditions are not uniform across the free-stream radiative path length. This nonuniformity violates the first assumption given in Section IV-B for application of the present line-ratio theory. Hence, some correction procedure may be required to obtain accurate free-stream temperature measurements.

Further measurements are suggested to determine the radial variation of 5106 and 5153 Å line intensities across the nozzle exit plane. These measurements would provide a firmer basis for making final conclusions about the radiative activity of the "cold" flow region with respect to copper line ratio measurements in the "hot" core of the nozzle free stream.

D. Line Shift

The above measurements of temperature and copper density required a correction for self-absorption effects. This correction implied that a theory was available for separating the broadening of copper lines due to self-absorption from ordinary line broadening and shift effects (i.e., collisions, doppler, natural, ..., etc.). However, a valid question is, what is the accuracy of this correction process? In Reference 8, various error sources are presented which can cause inaccuracies in the correction procedure. It was concluded that the self-absorption correction error was less than ± 7 percent for gas-cap temperature determination. However, there was no a priori way of determining if the Lindholm theory of collisional line broadening was correct for thermodynamic conditions encountered in the RENT environment. It was suggested that line shift and detailed line profile measurements might be used to corroborate the Lindholm theory for RENT flow application.⁽⁸⁾

Line shift measurements are a method of validating Lindholm's collision theory⁽⁷⁾ because the shift of copper lines in the RENT flow is due chiefly to collisional effects (i.e., collisions between copper atoms and other gas species). In Reference 8, it was further shown that Van der Waals broadening and shift was the most significant effect. Therefore, the following equation can be written⁽⁷⁾ for the shift, Δ_6 , of the lines in terms of Van der Waals broadening constant C_6 .

$$\Delta_6 = \Delta_6^0 + A C_6^{2/5} N_{NU} T^{3/10} [\text{\AA}] \quad (15)$$

where the Lindholm formulation gives

$$\Delta_6^0 = 0 \quad (16)$$

$$A = -1.10 \times 10^{-9}$$

C_6 is an empirical constant which has a unique value for each line, N_{NU} is the number density of neutral particles (i.e., atoms or molecules), and T is the gas temperature in $^{\circ}\text{K}$. Equation (15) implies that the shift of the copper lines is linearly proportional to the factor $N_{NU} T^{3/10}$ and has a slope which can be related to the broadening constant C_6 . The sign of

the constant, A, indicates that a red line shift will occur for both copper lines of interest.

Results of the 5106 and 5153 Å line shift measurements are shown in Figure 13 where the average shifts for all data records are plotted as a function of particular $N_{NU} T^{3/10}$ conditions. Also shown in this figure are error bars about the data points to designate the standard deviation of the shift data about this mean value. Note that three conditions are represented:

(1) Cu Calibration Lamp

$$N_{NU} \approx 0, T \approx 6000^\circ K$$

$$N_{NU} T^{3/10} \approx 0$$

(2) Free-Stream Conditions

$$N_{NU} = 2.8 \times 10^{19} \text{ particles/cm}^3, T = 5000^\circ K$$

$$N_{NU} T^{3/10} = 3.6 \times 10^{20} [\text{cm}^{-3} \text{ }^\circ K^{3/10}]$$

(3) Gas-Cap Conditions (i.e., Model Stagnation)

$$N_{NU} = 9.6 \times 10^{19} \text{ particles/cm}^3, T = 6500^\circ K$$

$$N_{NU} T^{3/10} = 13.3 \times 10^{20} [\text{cm}^{-3} \text{ }^\circ K^{3/10}].$$

Both pre- and post-run calibration shifts are shown with pre-run always set to zero. The variation between pre- and post-run calibration is therefore a measure of the repeatability of the position measurement as well as an indication of any slight grating rotation due to vibration of the measuring instrument.

Note that the measured line shifts tend to follow Lindholm's formulation given in Equation (15). The most serious deviation occurred in the measurement of the 5106 Å line for Run No. 91-020.⁽⁵⁾ Even though the slope of the line through the measurement points is in the proper direction, the data exhibits an anomalous overall "blue" shift which is not evident for latter tunnel runs. In Figure 4, it can be seen that for this particular run the 5106 line was located near the edge of the OMA screen. Perhaps the variation in screen output sensitivity in this region magnified a slight grating rotation, or that other nonlinear behavior occurred near edges of the OMA screen. At any rate, this anomaly did not appear in the remaining data taken with both lines located near the screen centerline.

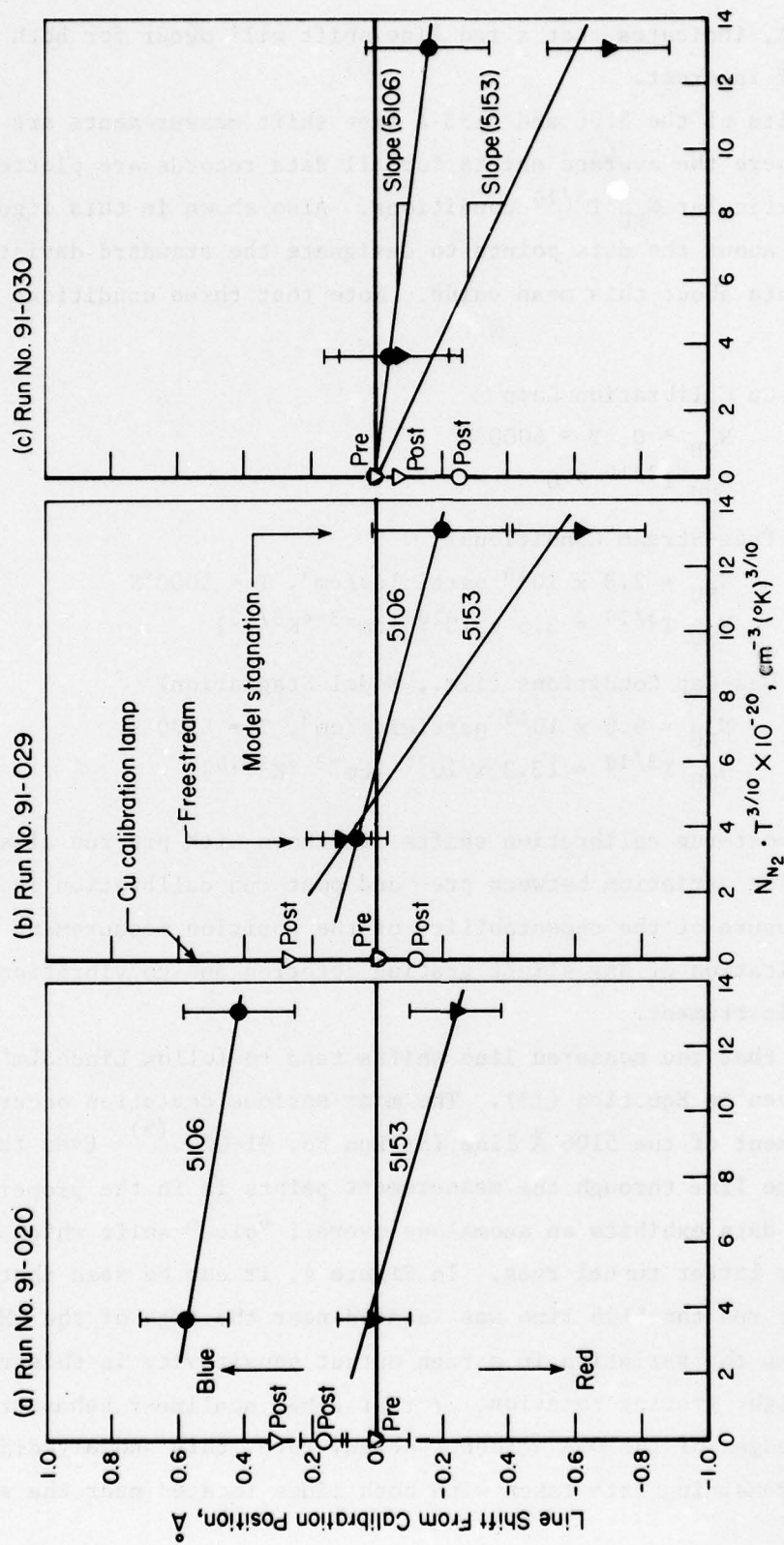


FIGURE 13. LINE SHIFT DATA FOR VARIOUS ARC-TUNNEL RUNS WHICH WERE USED TO INFER BROADENING CONSTANTS FOR THE COPPER LINES OF INTEREST

Specific values for the broadening and shift constants Δ_6^0 and C_6 taken from the shift data in Figure 13 are listed in Table 4. In Table 5, the average of the results for C_6 values for each line and the ratio of C_6 values for the two lines are compared with values measured by other experimenters. The arc-tunnel determined values of C_6 shown in Table 5 agree reasonably well with measurements by Ovechkin⁽⁹⁾ in a 1-atmosphere free-burning arc and with Calspan⁽⁶⁾ data for shock tube conditions similar to the RENT environment. This agreement tends to verify the use of Lindholm's theory to predict collision broadening in the RENT flow and lends credibility to the self-absorption correction method. More accurate line shift results in the RENT environment could ultimately lead to an improved accuracy for this important data correction procedure.

E. Detailed Line Shape

Besides the above line shift considerations, another method of examining the accuracy of temperature and copper density measurement results is to check for consistency in the theoretical procedure of correcting for self-absorption effects. This is accomplished by comparing the entire measured 5106 and 5153 Å line profile shapes against the theoretical profiles determined using only the peak intensity ratio and the 5106 Å line width. For instance, other measured variables of interest, which should also agree with theoretical predictions, are the 5153 Å line full half-width, and the integrated line intensity ratio. The above line profile comparisons are shown in Figures 14 and 15 for various experimental conditions.

Note that for the free-stream environment (i.e., Figure 14a) the entire theoretical profile shape for a temperature of 5250 K and a copper density of $3 \times 10^{15} \text{ cm}^{-3}$ agrees well with the measured shape for both lines of interest. This was not altogether unexpected since the actual line full-widths were narrow compared to the instrument apparatus function widths for these experimental conditions so that changes in the true line width tended to be masked and the measured profiles therefore resembled the apparatus function shapes instead of the actual profile shapes. For the case of model stagnation conditions, the measured line shapes are more

TABLE 4. BROADENING CONSTANTS DETERMINED FROM
SHIFT DATA FOR EACH TUNNEL RUN

Run No.	Line, Å	C ₆ , cm ⁶ /sec	$\frac{C_6(5153)}{C_6(5106)}$	Δ_6^0 , Å
91-020	5106	-0.9×10^{-32}	3	+0.64
	5153	-0.3×10^{-31}		+0.10
91-029	5106	-2.5×10^{-32}	11	+0.15
	5153	-2.8×10^{-31}		+0.32
91-030	5106	-0.5×10^{-32}	24	+0.00
	5153	-1.1×10^{-31}		-0.01

$$\Delta_6 = \Delta_6^0 - 1.10 \times 10^{-9} C_6^{2/5} N_{NU} T^{3/10}, \text{ Å}$$

TABLE 5. AVERAGE BROADENING CONSTANTS DETERMINED FROM ALL ARC-TUNNEL DATA COMPARED TO VALUES DETERMINED BY OTHER AUTHORS

Line	\bar{C}_6 , cm ⁶ /sec	$\frac{\bar{C}_6(5153)}{\bar{C}_6(5106)}$
5106	$-1.3 \times 10^{-32} \pm 1.1 \times 10^{-32}$	13 ± 10
5153	$-1.4 \times 10^{-31} \pm 1.3 \times 10^{-31}$	

$$C_6(\text{Ovechkin})^{(9)} = \begin{aligned} &-1 \times 10^{-32} (5106) \\ &-1 \times 10^{-31} (5153) \end{aligned}$$

$$C_6(\text{Calspan})^{(6)} = -1.7 \times 10^{-32} (5106)$$

$$\frac{C_6(5153)}{C_6(5106)} = 10 (\text{Ovechkin})^{(9)}$$

$$\Delta_6^0(\text{Theory}) = 0$$

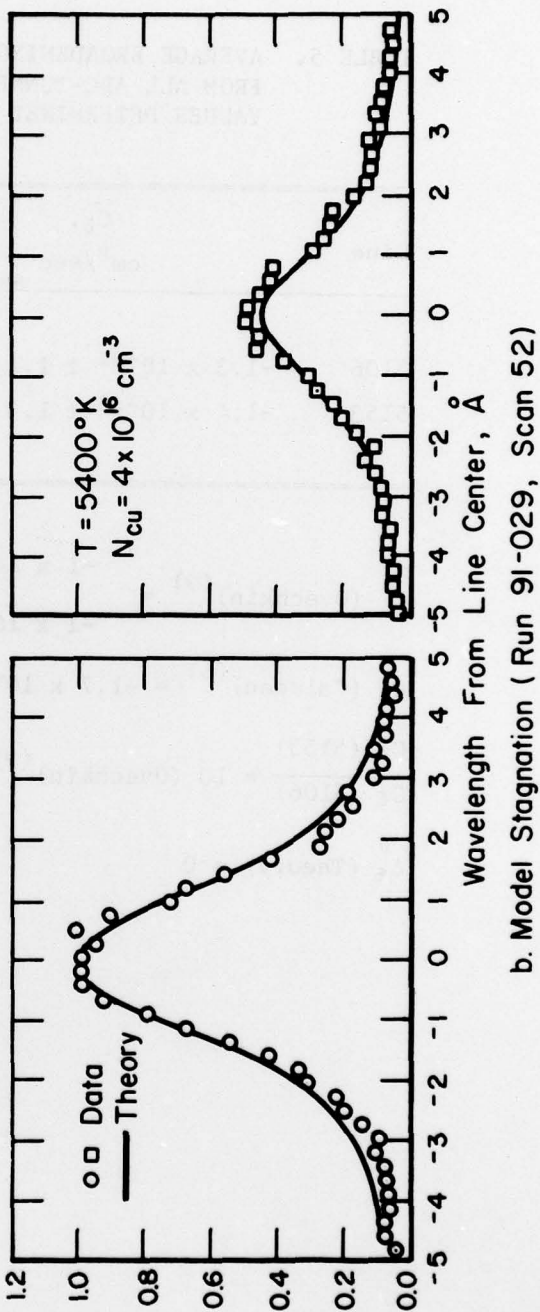
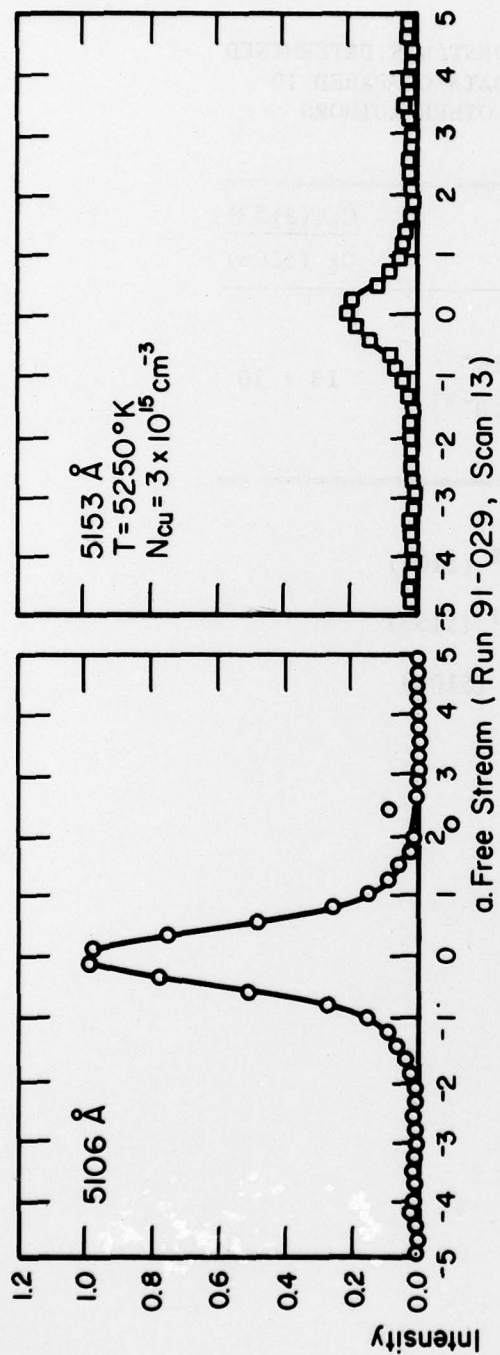


FIGURE 14. COMPARISON OF OMA DATA SCANS WITH THEORY FOR FREE-STREAM VERSUS MODEL STAGNATION CONDITIONS

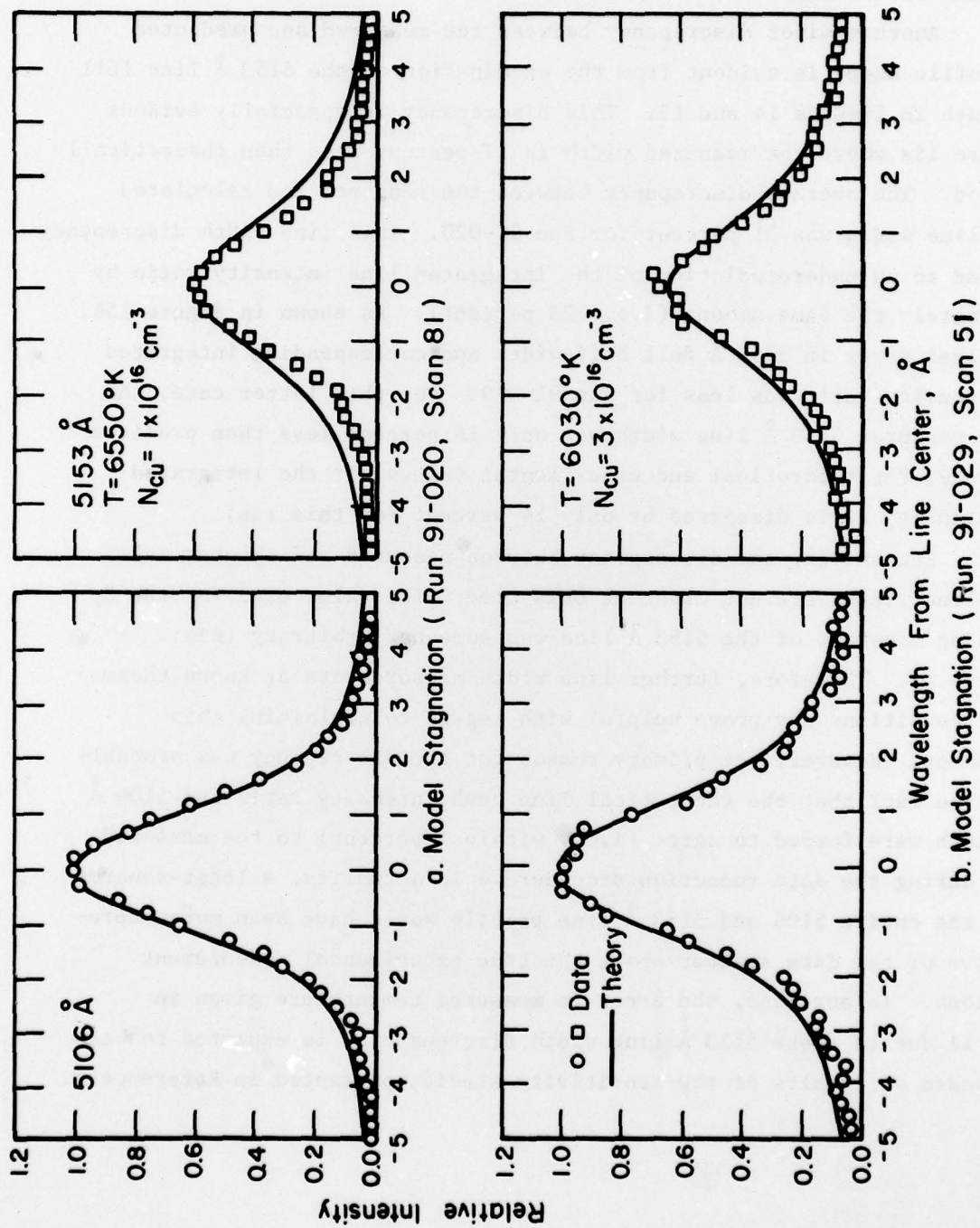


FIGURE 15. COMPARISON OF OMA DATA SCANS WITH THEORY FOR TYPICAL MODEL STAGNATION CONDITIONS

indicative of actual conditions, and small discrepancies between theory and experimental data can be noted. In Figure 14b as well as in Figures 15a and 15b, the theory predicts a less rapid fall-off in the 5106 Å line intensity near the wings of the line than was measured in the arc-tunnel environment.

Another minor discrepancy between the measured and predicted line profile shape is evident from the examination of the 5153 Å line full half-width in Figures 14 and 15. This discrepancy is especially evident in Figure 15a where the measured width is 17 percent less than theoretically predicted. The average discrepancy between the measured and calculated 5153 Å line width was 21 percent for Run 91-020. This line width discrepancy also lead to an underprediction of the integrated line intensity ratio by approximately the same amount (i.e., 23 percent). As shown in Figure 15b, the typical error in 5153 Å full half-width and corresponding integrated line intensity ratio was less for Run 91-029. For this latter case, the average measured 5153 Å line width was only 16 percent less than predicted and, hence, the theoretical and experimental values for the integrated line intensity ratio disagreed by only 14 percent for this run.

Reasons for the discrepancy between measured and theoretical 5153 Å line widths are not clear at this time. The value used for the C_6 broadening constant of the 5153 Å line was somewhat arbitrary (see Reference 8). Therefore, further line width measurements at known thermodynamic conditions may prove helpful with regard to explaining this discrepancy. However, the primary reason for the discrepancy was probably due to the fact that the theoretical line peak intensity ratio and 5106 Å line width were forced to agree (i.e., within 1 percent) to the measured values during the data reduction procedure. In actuality, a least-squares fit of the entire 5106 and 5153 Å line profile would have been more representative of the data scatter about the true experimental measurement conditions. In any case, the error in measured temperature given in Figure 11 due to these 5153 Å line width discrepancies is expected to be small based on results of the sensitivity studies presented in Reference 8.

F. Polychromator Considerations

Previous attempts to measure the flow enthalpy in the RENT facility utilized a polychromator apparatus with four fixed slits to monitor integrated 5106 Å and 5153 Å line intensities.^(3,4,12) This was accomplished by measuring the background intensities near these lines with two polychromator channels and the line intensity plus background with the other two, then electronically subtracting the background signal to obtain the true integrated line intensity values. This procedure assumes that the actual line widths are narrower than the polychromator slit apparatus function widths and that line shifts are small. To examine these assumptions, the true self-absorption broadened line shapes were computed for typical conditions obtained during Runs 91-029 and 91-030. Also, the average line shifts were superimposed on these profiles. Results of these calculations are shown plotted in Figure 16 where the intensity of both lines was normalized to 1. Also shown in Figure 16 is the polychromator apparatus function used in References 3, 4, and 12. Note that the polychromator apparatus function width is of the same order as the measured line widths obtained in the present study, which results in intensity measurement losses in the line wings. Also note that the measured line shifts are also comparable to this apparatus function width which indicates that errors in integrated line intensity ratio and the absolute intensity of the 5106 Å line will result if a fixed slit polychromator positioned with a low-pressure copper calibration source prior to the arc-tunnel run is utilized as the spectral measurement device.

Despite the error sources noted above, the Polychromator Method has several advantages over the OMA technique. Presently, the OMA is limited to approximately five data points per second while the polychromator can continuously sample the spectrum of interest. This continuous data gathering capability would provide more information on variations in stagnation temperature during a particular model dwell time. Also, the polychromator approach is more amenable to on-line, real-time display of stagnation enthalpy using analog devices to reduce the four-channel output.

Hence, a combination of the two techniques might be most appropriate. The polychromator apparatus function could be preshifted

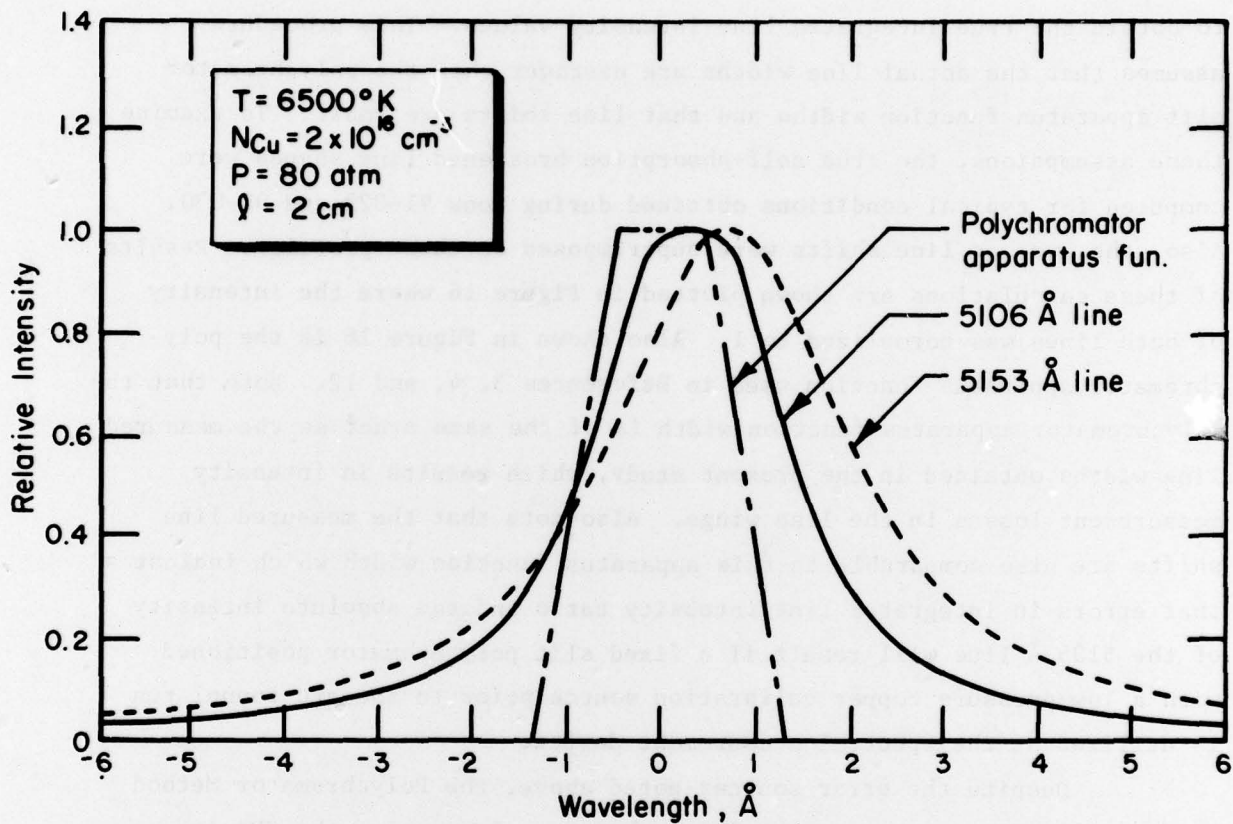


FIGURE 16. INDICATION OF POLYCHROMATOR PERFORMANCE FOR AVERAGE
 LINE SHIFT AND SHAPE CONDITIONS DURING RUNS 91-029
 AND 91-030

for each line using the copper hollow-cathode lamp and the OMA to accurately guide the adjustment of polychromator slit positions. The accuracy of this position setting is estimated to be within $\pm 0.1 \text{ \AA}$ of the expected line shift. The apparatus function could also be broadened, especially at the base, in order to more nearly correspond to the expected line shape during arc-tunnel operation. Simultaneous OMA and polychromator data would then be obtained with the OMA data being primarily used to verify that the predicted shift and shape changes were, in fact, realized. Both methods could then be used to obtain stagnation temperature corrected for self-absorption. Either the measured copper density determined from the OMA line-shape results or the polychromator output for the continuous absolute 5106 line intensity could be used to correct the polychromator data for self-absorption effects. If the preset shifts were incorrect for a particular tunnel run, then the OMA data alone would suffice to indicate the average stagnation temperature for a particular model test.

For free-stream measurements, no real advantage would be gained in the speed of the polychromator approach over the OMA method of data gathering. However, real-time display of results would continue to remain important.

VI. SUMMARY AND CONCLUSIONS

The text of this report contains results of free-stream and model stagnation temperature measurements in the RENT arc-facility for a parallel-flow nozzle operating in the "high-swirl" mode. These results were obtained through analysis of detailed, high-resolution spectra of the 5106 and 5153 Å copper lines. Besides line intensity data, these spectra also yielded valuable line shift and shape information which was used to validate the data reduction procedure. A modified Copper-Line-Intensity-Ratio Method was utilized in the data reduction process, which corrected the simple line ratio for self-absorption effects. This correction procedure involved the simultaneous measurement of the 5106 Å line full half-width in order to infer flow copper number density. Hence, the present data represent the most accurate spectroscopically determined values of flow enthalpy that have been obtained to date. Based on these results and theoretical considerations, the following specific conclusions are applicable:

- (1) Free-stream copper density measurements indicated that this particular flow regime was nearly optically thin for typical "high-swirl" RENT operating conditions.
- (2) The average corrected free-stream temperature was 5360 K which does not differ much from the average optically thin value of 5720 K. This agreement indicates that, indeed, free-stream self-absorption effects are small.
- (3) Line intensity measurements and theoretical calculations indicated that the radial temperature (i.e., enthalpy) spike present in the RENT "high-swirl" nozzle exit flow can introduce errors in the free-stream temperature measurements. Further tests are required to quantify this error source.

- (4) Similar measurements and calculations imply that the model gas-cap radiation will not be affected by the "cold" free-stream flow around the bow shock wave. Hence, the assumption of a radiatively inactive free stream is valid for gas-cap copper line ratio measurements.
- (5) Reduced copper emission data showed that the average measured stagnation point copper density was two orders of magnitude greater than the maximum amount present in an optically thin flow. Hence, self-absorption cannot be ignored for the RENT model gas-cap environment.
- (6) The corresponding average corrected model stagnation temperature was 6470 K, which was 11 to 38 percent lower than that determined using a simple optically thin analysis. This disagreement confirms the necessity of including a self-absorption correction for model stagnation conditions.
- (7) The average corrected ratio of free-stream temperature to model stagnation temperature was within 9 percent of that predicted using a simple isentropic flow analysis for a constant ratio of specific heats of 1.2. Also, the measured ratio of copper density (i.e., average flow density) across the bow shock wave was 23 percent higher than that inferred from these same theoretical calculations. This reasonable comparison between theory and experiment demonstrates the consistency of corrected copper line results for vastly different flow conditions.
- (8) The corrected average enthalpy measurement was 5250 Btu/lbm with a ± 15 percent fluctuation about this average for the RENT "high-swirl" condition. This mean value was 22 to 85 percent

lower than that inferred from optically thin temperature results. The large enthalpy correction reaffirms the necessity for including self-absorption effects in the data reduction procedure for model gas-cap conditions.

- (9) Errors associated with the above enthalpy measurement were estimated to be ± 12 percent of the mean value (see Reference 8 for details). This error estimate included the self-absorption correction only. Other error sources (i.e., nonuniformity and nonequilibrium, etc.) may increase the above error estimate as these effects are quantitatively examined.
- (10) The average enthalpy of 5250 Btu/lbm determined from the line-ratio technique is in excellent agreement with an average value of 5350 Btu/lbm which was determined from heat flux and pitot probe data using laminar heating relationships⁽¹³⁾. Also, the ± 15 percent fluctuation in measured enthalpy from the copper line ratio method is in good agreement with the ± 20 percent fluctuation estimate given in Reference 13.
- (11) Line shift results, which are independent of flow copper density, indicated that Van der Waals broadening was the dominant line broadening mechanism in the RENT free-stream environment. For gas-cap conditions, the Van der Waals line width again dominated along with self-absorption broadening of the copper lines of interest. Van der Waals constants determined from these line shift measurements were in good agreement with those measured in other high-temperature environments. This agreement tends to support the present use of Lindholm's theory to correct for self-absorption effects in the RENT environment.

- (12) The high-resolution line shape profiles obtained during this study show that the measured line contours are also in good agreement with predictions based on Lindholm's line broadening theory. As with the line shift results, the line contour measurements do not conclusively prove that Lindholm's theory is completely applicable to the RENT environment. However, the consistency of these line shape and line shift results certainly lends support to the argument that Lindholm's formulation for collision broadening does, in fact, satisfy the requirement for a method of accurately correcting for self-absorption effects for RENT gas-cap conditions.
- (13) Line shape and shift results obtained in this study indicate that a polychromator apparatus cannot be used alone to obtain accurate line intensity data in the RENT gas-cap environment. The OMA is required, in conjunction with the polychromator, to preshift and adjust the polychromator apparatus function position to better enable this instrument to obtain true integrated line intensity data. The OMA output is also required to check that the pre-shifted position values are valid during the actual tunnel run and to obtain an independent measure of the copper number density and temperature during the test.

REFERENCES

- (1) Lawrence, L. R., Jr., Walterick, R. E., Weeks, T. M., and Doyle, J. P., Jr., "Total Enthalpy Measurement from Blunt Body Gas-Cap Emission in Arc-Heated Wind Tunnels: Results and Application", AFFDL-TM-72-22 FX (1972), also AIAA Paper No. 72-1021 presented at AIAA 7th Aerodynamic Testing Conference, Palo Alto, California (September, 1972).
- (2) Bader, J. B., "Time Resolved Absolute Intensity Measurements of the 5106 Å Copper Atomic Spectral Line in the AFFDL RENT Facility", AFFDL-TR-75-33 (June, 1975).
- (3) Bader, J. B., "Development of an Electronics Package for Use in Real-Time, Optically Thin, Isothermal Spectral Line Intensity Ratio Temperature Measurements", AFFDL-TR-74-153 (June, 1975).
- (4) Bader, J. B., Unpublished work at AFFDL.
- (5) Boiarski, A. A., "Detailed Measurements of Line Shape, Line Shift, and Self-Absorption Effects on Stagnation Enthalpy Measurements Using the Copper-Line-Intensity-Ratio Technique", AFFDL-TM-78-33-FXN (February, 1978).
- (6) Boyer, D. W., et al, "Relative Transition Probabilities and Pressure Broadening Parameters of Copper Atomic Lines", AFFDL-TR-78-82, 1978.
- (7) Lindholm, E., "Pressure Broadening of Spectral Lines", Arkiv for Matematik, Astronomi och Fysik, Bd 32 A., No. 17 (1946).
- (8) Boiarski, A. A., "Methodology for Making a Self-Absorption Correction to the Simple Copper-Line-Ratio Technique Used for Arc-Tunnel Enthalpy Measurements", AFFDL-TR-79-XX, 1979, to be published.
- (9) Ovechkin, G. V., and Sandrigailo, L. E., "Line Broadening and Shift in an Arc for Low Copper Contents", J. Appl. Spec. (USSR), 10, 4, p. 565 (1969).
- (10) Neel, C. A., and Lewis, C. H., "Interpolations of Imperfect Air Thermodynamic Data II., at Constant Pressure", AEDC-TDR-64-184 (September, 1964).
- (11) Beachler, J. C., "Operating Characteristics of the Air Force Flight Dynamics Laboratory Reentry Nose Tip (RENT) Facility", Presented at the ASTM/IES/AIAA 5th Space Simulation Conference, Gaithersburg, Maryland, September, 1970.
- (12) Brown-Edwards, E. G., "Comparison and Evaluation of Several Experimental Techniques for Local Enthalpy Measurements in an Arc-Heated, High-Pressure, Supersonic Air Flow", AFFDL-TR-77-35 (1977).
- (13) "Reentry Nose Tip, Air Force Flight Dynamics Laboratory Information Manual for Users", 4th Edition, March, 1977.